Phys. Lett. B 870 (2025) 139898

Contents lists available at ScienceDirect

Physics Letters B

journal homepage: www.elsevier.com/locate/physletb

Letter

Constraining off-shell Higgs boson production and the Higgs boson total width using $WW \to \ell\nu\ell\nu$ final states with the ATLAS detector

The ATLAS Collaboration[1]

ARTICLE INFO

Editor: Dr. M. Doser

ABSTRACT

A measurement of off-shell Higgs boson production is performed in the $H^* \to WW$ channel. The measurement uses a proton–proton collision dataset with an integrated luminosity of 140 fb^{-1} collected at a centre-of-mass energy of 13 TeV by the ATLAS detector at the Large Hadron Collider. Final states in which both W bosons decay leptonically are targeted, and events are categorised based on the flavour of the final-state leptons, the jet multiplicity, and the output of neural network-based classifiers. The data are found to be compatible with the Standard Model expectation. An observed (expected) upper bound on the 95 % symmetric confidence level interval is set on the rate of off-shell Higgs boson production at a value of 3.4 (4.4) times the Standard Model prediction. These results are combined with the results from the measurement of on-shell Higgs boson production in the same final states to obtain an observed (expected) upper bound at 95 % confidence level on the Higgs boson total width of 13.1 (17.3) MeV.

1. Introduction

Since its discovery in the year 2012 by the ATLAS [1] and CMS [2] Collaborations, the Higgs boson has been at the centre of a major campaign of searches and measurements. These efforts aim to test the compatibility of the Higgs boson's properties with the Standard Model (SM) predictions. No significant discrepancies have been found to date, but the current precision of the measurements leaves substantial room for beyond-the-SM (BSM) effects for several parameters, for example the total width of the Higgs boson, Γ_H.

As Γ_H represents the sum of the partial widths of the individual decay modes of the Higgs, any modification caused by an additional BSM interaction would impact its value. Values of the Higgs boson width either above or below the SM prediction occur in various formulations of BSM physics, including composite Higgs models [3], two-Higgs-doublet models [4], and various scalar extensions of the SM [5]. Therefore, a precise measurement of Γ_H may provide sensitivity to BSM physics.

In the SM, the Higgs boson width can be computed using the known masses and couplings of all particles to which the Higgs boson decays, which yields a value of 4.1 MeV with an associated uncertainty of approximately 1 % [6]. Due to the limited resolution of the ATLAS and CMS detectors, a direct measurement of the width from the Higgs boson mass peak [7,8] cannot reach the MeV-scale precision needed to probe this quantity experimentally. However, this level of precision can be achieved through an indirect method proposed in Refs. [9–11], which uses Higgs boson decays to pairs of vector bosons VV, where $VV = WW$ or ZZ. This method compares the rates of Higgs boson production measured across two parts of the phase space distinguished by the invariant mass of the vector boson pair, m_{VV}: when m_{VV} is close to the Higgs boson pole mass, m_H (on-shell regime), and when m_{VV} is much greater than that value (off-shell regime).[2] The rate of VV production mediated by an on-shell Higgs boson H depends on the Higgs boson's couplings to particles in its production and decay, $g_{\text{prod}}(m_H)$ and $g_{\text{decay}}(m_H)$, as well as its total width, Γ_H. In contrast, the rate of VV production mediated by an off-shell Higgs boson H^* is independent of the total width but still depends on the couplings $g_{\text{prod}}(\hat{s})$ and $g_{\text{decay}}(\hat{s})$, where $\hat{s}$ represents the virtuality of the Higgs boson.

Deviations from the SM predictions for these rates can be expressed in terms of the on-shell and off-shell signal strengths, $\mu_{\text{on-shell}}$ and $\mu_{\text{off-shell}}$, as follows:

$$\begin{aligned} \mu_{\text{on-shell}} &= \kappa^2_{\text{prod,on-shell}} \cdot \kappa^2_{\text{decay,on-shell}} \cdot \frac{1}{\kappa_H}; \\ \mu_{\text{off-shell}} &= \kappa^2_{\text{prod,off-shell}} \cdot \kappa^2_{\text{decay,off-shell}}, \end{aligned} \tag{1}$$

where $\kappa_H = \Gamma_H/\Gamma_H^{\text{SM}}$, and the other κs represent coupling strength modifiers with respect to the SM predictions, $\kappa_i = g_i/g_i^{\text{SM}}$, where i = prod or decay. Assuming that the coupling strength modifiers are the same for both regimes, $R_i = \kappa^2_{i,\text{off-shell}}/\kappa^2_{i,\text{on-shell}} = 1$, the total Higgs boson width can be extracted by taking the ratio of measured on-shell and off-shell

[1] Authors are listed at the end of this paper.

[2] In this analysis the threshold between on-shell and off-shell production is set to $m_{VV} = 140$ GeV as defined in Ref. [6].

https://doi.org/10.1016/j.physletb.2025.139898
Received 11 April 2025; Received in revised form 15 September 2025; Accepted 16 September 2025
Available online 3 October 2025

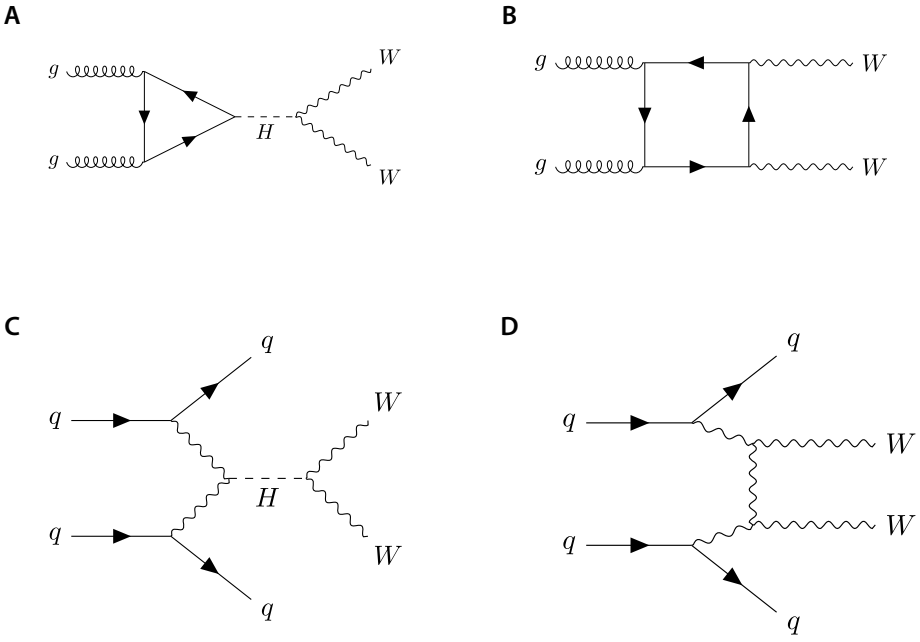

Fig. 1. Example diagrams of leading-order gluon-induced WW production (ggF) (a) including and (b) not including a Higgs boson, and quark-induced WW production (EW) (c) including and (d) not including a Higgs boson.

signal strengths.[3] Experimentally, this method is feasible because off-shell production in $H^* \to VV$ channels is enhanced for invariant masses m_{VV} above $2m_V$, as the vector bosons themselves become on-shell. This effect partially compensates the rapid decrease in the rate of Higgs boson production that occurs away from its mass peak.

Evidence for off-shell Higgs boson production in the $H^* \to ZZ$ channel has been reported by both the CMS and ATLAS Collaborations, using the full LHC Run 2 data set in the 4ℓ and $2\ell 2\nu$ final states, where ℓ denotes an electron or muon. The ATLAS Collaboration published an analysis employing neural simulation-based inference [14], yielding $\Gamma_H = 4.3^{+2.7}_{-1.9}$ MeV with a significance of 3.7σ. The CMS Collaboration presented a significance of 3.8σ, corresponding to a constraint of $\Gamma_H = 3.0^{+2.0}_{-1.5}$ MeV [7,15]. Another strategy to measure Γ_H, which relies on the measurement of the production of four top quarks, was recently performed by the ATLAS Collaboration leading to an upper limit on Γ_H of 450 MeV [16]. The latest published results from the $H^* \to WW$ channel are from 2015 [17] and 2016 [18], by the ATLAS and CMS Collaborations, respectively. The $H^* \to WW$ channel provides an opportunity for an independent measurement of off-shell Higgs boson production and the Higgs boson width, and it offers a larger sample of events than $H^* \to ZZ$, reducing statistical limitations. Studying this channel is also particularly relevant as BSM scenarios may affect $H \to WW$ and $H \to ZZ$ differently. In particular, models that violate custodial symmetry, including scalar extensions of the Standard Model (e.g., multi-Higgs doublet models [19]), can introduce deviations between these channels, making it essential to analyze both in order to fully probe new physics effects [20,21]. However, the $H^* \to WW$ channel also carries additional challenges: the fully-leptonic final state of the $H^* \to WW$ channel has substantially higher backgrounds than the $H^* \to ZZ \to 4\ell$ channel, and selections on the mass of the vector bosons are less effective than in both the $H^* \to ZZ \to 2\ell 2\nu$ and $H^* \to ZZ \to 4\ell$ channels due to the presence of neutrinos in both W decays.

This paper presents the first LHC Run 2 measurement of off-shell Higgs boson production in the fully leptonic final state of the $H^* \to WW$ channel. It also provides the first standalone $H^* \to WW$ interpretation of Γ_H by the ATLAS experiment. The analysis considers Higgs boson production via gluon-gluon fusion (ggF), $gg \to H^* \to WW$, and electroweak (EW), $qq \to H^* \to WWjj$, production modes. In the off-shell regime, the interference of these processes with non-resonant backgrounds that share the same initial and final states, $gg \to WW$ and $qq \to WWjj$ respectively, is large. The full process in each production mode, including the Higgs-mediated signal, the background, and the interference terms, is referred to as $gg \to (H^* \to)WW$ and $qq \to (H^* \to)WWjj$, respectively. Example Feynman diagrams for these processes are shown in Fig. 1. Due to the predominantly destructive nature of the interference in the phase space considered in this analysis, the presence of off-shell Higgs boson production is characterized by a deficit in the number of events relative to the background-only hypothesis.

The analysis considers both different-flavour (DF, $H^* \to WW \to e\nu_e\,\mu\nu_\mu$) and same-flavour (SF, $H^* \to WW \to e\nu_e e\nu_e$, $\mu\nu_\mu\mu\nu_\mu$ leptonic final states, including cases where the W bosons decay via intermediate τ leptons, introducing one additional τ-neutrino in the final state. Events are categorized based on the decay mode (DF or SF) and the number of jets, N_j (0, 1, or ≥2), leading to six distinct analysis regions, each with a dedicated event selection. A classification neural network (DNN) is trained for each region to discriminate against non-interfering backgrounds, and in each region events are divided into three categories based on the DNN score. To enhance sensitivity to the interference effects, an additional variable, V_{31}, is reconstructed in each of these categories. Defined as a combination of the dilepton invariant mass and the transverse mass of the dilepton-plus-missing-energy system, V_{31} serves as a proxy for the non-reconstructable true ("particle-level") invariant mass of the WW system, m_{WW}. A likelihood fit to this variable across all regions and categories is performed to extract the off-shell Higgs boson production signal strength. Finally, a combined fit of this off-shell analysis with the corresponding on-shell measurement [22], using the same final state and data-set, is used to constrain Γ_H.

2. ATLAS detector

The ATLAS experiment [23] at the LHC [24] is a multipurpose particle detector with a forward–backward symmetric cylindrical geometry

[3] This assumption may be violated in some BSM theories, including the Georgi-Machacek (GM) model [12] and particular Sigma models [13].

and a near 4π coverage in solid angle.[4] It consists of an inner tracking detector (ID) surrounded by a thin superconducting solenoid providing a 2 T axial magnetic field, electromagnetic and hadronic calorimeters, and a muon spectrometer. The ID covers the pseudorapidity range $|\eta| < 2.5$. It consists of silicon pixel, silicon microstrip, and transition radiation tracking detectors. Lead/liquid-argon (LAr) sampling calorimeters provide electromagnetic (EM) energy measurements with high granularity within the region $|\eta| < 3.2$. A steel/scintillator-tile hadronic calorimeter covers the central pseudorapidity range ($|\eta| < 1.7$). The endcap and forward regions are instrumented with LAr calorimeters for EM and hadronic energy measurements up to $|\eta| = 4.9$. The muon spectrometer surrounds the calorimeters and is based on three large superconducting air-core toroidal magnets with eight coils each. The field integral of the toroids ranges between 2.0 and 6.0 T m across most of the detector. The muon spectrometer includes a system of precision tracking chambers up to $|\eta| = 2.7$ and fast detectors for triggering up to $|\eta| = 2.4$. The luminosity is measured mainly by the LUCID–2 [25] detector, which is located close to the beampipe. A two-level trigger system is used to select events [26]. The first-level trigger is implemented in hardware and uses a subset of the detector information to accept events at a rate close to 100 kHz. This is followed by a software-based trigger that reduces the accepted rate of complete events to 1.25 kHz on average depending on the data-taking conditions. A software suite [27] is used in data simulation, in the reconstruction and analysis of real and simulated data, in detector operations, and in the trigger and data acquisition systems of the experiment.

3. Data and simulated events

3.1. Data samples

This analysis uses proton–proton (pp) collision events collected at a centre-of-mass energy of 13 TeV between the years 2015 and 2018, with either a single-electron or single-muon trigger [28–30]. The transverse momentum, p_{T}, thresholds for both electron and muon triggers were set to 26 GeV for the majority of Run 2, except the first year where the thresholds were 24 and 20 GeV for electron and muon triggers, respectively. Events are only selected for further analysis if they pass "good-for-physics" quality criteria, meaning primarily that the relevant detector components are in good operating condition (see Ref. [31] for an exact definition). The total integrated luminosity of the collected dataset is 140 fb^{-1} with an uncertainty of 0.83 % [25,32].

3.2. Simulated samples

This section describes the simulation of the pp collisions for all the processes used in the analysis. For all processes containing a Higgs boson, the mass of the Higgs boson was set to 125 GeV in the generation, and samples were normalised to cross sections computed for a mass of 125.09 GeV [33].

The dominant ggF off-shell Higgs boson signal process ($gg \to H^* \to WW$, ggF S), the interfering gluon-induced background process ($gg \to WW$, ggF B), and the full process including interference ($gg \to (H^* \to) WW$, ggF SBI) were each generated at leading order (LO) in QCD with up to one additional parton in the final state using Sherpa 2.2.2 [34] and OpenLoops [35–38]. The ggF S, ggF B and ggF SBI processes were separately corrected to next-to-leading order (NLO) in QCD as a function of the generator-level m_{WW} according to the following steps. First, NLO/LO corrections were derived at fixed order in QCD as a function of m_{WW} using Powheg Box v2 [39–41] as in Ref. [42]. The corrections generally decrease as a function of m_{WW}, amounting to around 100 % at 200 GeV, and flattening out to around 50 % from 400 GeV onwards. Second, these corrections were applied to LO MC samples generated using MadGraph5 [43] and showered using Pythia 8.2 [44]. Lastly, the m_{WW} spectrum of the Sherpa samples was reweighted to match the corrected MadGraph5 spectrum. This method is necessary because the fixed-order NLO/LO corrections derived with Powheg Box v2 do not apply fully to the merged Sherpa samples. The stepwise approach preserves the per-event kinematic information of the Sherpa samples, while correcting its m_{WW} spectrum differentially to NLO. Two further constant higher-order QCD corrections were applied to the above ggF samples: a factor 1.2 next-to-NLO (NNLO)/NLO correction [45–47], and a factor 1.1 next-to-NNLO (N^{3}LO)/NNLO correction [48]. The former was derived for the Higgs-mediated process, while the latter was derived for a region of phase space where the on-shell component dominates. Corrections that apply more closely to the phase space or samples considered here are not available, so these corrections were applied uniformly for ggF S, ggF B and ggF SBI.

Following ggF, the next largest source of off-shell Higgs boson production is through EW processes. These include vector boson fusion (VBF) and the associated production of a vector boson and an off-shell Higgs boson (VH^*), with vector boson decays to quark anti-quark pairs. Four samples were generated to model the EW contribution: the full process including both the signal and its interfering background ($qq \to (H^* \to) WWjj$, EW SBI), a variant of this process with $\mu_{\text{off-shell}}$ and the Higgs boson width both scaled by a factor of 20 relative to the SM (EW SBI20), the interfering background alone ($qq \to WWjj$, EW B), and the signal process excluding the contribution from the t-channel Higgs boson diagram ($qq \to H^* \to WWjj$, EW S). Generating a complete signal-only sample is not possible because some diagrams contributing to the EW process lack an s-channel Higgs exchange, making it impossible to apply the usual high transverse mass requirement to ensure the Higgs boson is off-shell. Therefore, the EW S sample was used solely for training the neural network as described in Section 5. Combinations of the EW SBI20, EW SBI and EW B samples allow the signal, background and interference components to be accounted for in the full parameterization of the event yield, which is further detailed in Section 8. For each of these samples, the hard scattering process was generated by MadGraph5 at LO in QCD and EW and the NNPDF3.0nlo [49] set of parton distribution functions (PDFs) was used. The parton shower, hadronisation and underlying event were modelled using Pythia 8.2 with the dipole-recoil scheme and A14 set of tuned parameters (tune) [50]. NLO corrections for the EW contributions exist [51], but they are calculated for a different phase space to the one used in this analysis, and are therefore not used.

On-shell Higgs boson production in the $H \to WW^*$ channel was modelled for ggF, VBF, VH and $t\bar{t}H$. The small backgrounds due to on-shell $H \to \tau\tau$ decays were also modelled for the ggF, VBF and VH production modes. In both cases, production via ggF was modelled at NNLO in QCD using Powheg NNLOPS [52] and normalised to N^{3}LO in QCD and NLO in EW [6]. Both VBF and VH modes were generated with Powheg Box v2 at NLO in QCD and normalised to NNLO QCD and NLO EW [6,53,54]. The $t\bar{t}H$ mode was modelled using the Powheg Box v2 [52,55] generator at NLO and normalised to a cross section calculated at NLO in QCD and NLO in EW accuracy [6]. The on-shell production modes were interfaced to Pythia 8.212 (for ggF and VH) or Pythia 8.230 (for VBF and $t\bar{t}H$) for parton showering and hadronisation, with parameters set according to the AZNLO [56] (for ggF, VBF, and VH) or A14 (for $t\bar{t}H$) tunes. The samples use the PDF4LHC15$_{\text{NNLO}}$ [57] (for ggF, VBF, and VH) or NNPDF3.0$_{\text{NLO}}$ (for $t\bar{t}H$) PDF sets.

Fully-leptonic diboson (WW, ZZ, WZ, and $V\gamma^*$) and $V\gamma$ processes were generated with Sherpa 2.2.12 and 2.2.8 respectively, while

[4] ATLAS uses a right-handed coordinate system with its origin at the nominal interaction point (IP) in the centre of the detector and the z-axis along the beam pipe. The x-axis points from the IP to the centre of the LHC ring, and the y-axis points upwards. Polar coordinates (r, ϕ) are used in the transverse plane, ϕ being the azimuthal angle around the z-axis. The pseudorapidity is defined in terms of the polar angle θ as $\eta = -\ln\tan(\theta/2)$ and is equal to the rapidity $y = \frac{1}{2}\ln\left(\frac{E+p_z}{E-p_z}\right)$ in the relativistic limit. Angular distance is measured in units of $\Delta R \equiv \sqrt{(\Delta\eta)^2 + (\Delta\phi)^2}$.

semi-leptonic final states for ZZ and WZ were generated with SHERPA 2.2.11. The samples are accurate at NLO in QCD for up to one jet and LO in QCD for up to three jets. Loop induced $gg \to ZZ$ events including the off-shell Higgs boson signal, background and interference were generated at LO in QCD with up to one additional parton emission using SHERPA 2.2.2, for fully-leptonic and semi-leptonic final states. Triboson (VVV) processes were modelled by SHERPA 2.2.2 using factorised gauge-boson decays, and are accurate at NLO in QCD inclusively and LO for up two additional jets.

Events containing a vector boson and jets (V + jets) were simulated using SHERPA 2.2.11 (for ee and $\mu\mu$ final states) and SHERPA 2.2.14 (for $\tau\tau$ final states). The simulations are accurate at NLO in QCD for up to two jets and LO in QCD for up to five jets and are calculated in the five-flavour scheme using COMIX [58]. The samples were normalised to cross sections computed at NNLO in QCD [59].

For all SHERPA samples, the matrix element calculations were matched and merged with the SHERPA parton shower based on Catani-Seymour dipole factorisation [58,60] using the MEPS@NLO prescription [61–64] and the default tuning parameters. Virtual QCD NLO corrections were provided by the OPENLOOPS library. The NNPDF3.0$_{\text{NNLO}}$ set of PDFs was used, along with the dedicated set of tuned parton shower parameters developed by the SHERPA authors. For WW and V + jets samples, approximate NLO EW corrections were applied following the additive approach [65].

Electroweak Z production in association with two jets (EW Zjj) was generated using Herwig 7.1.3 and HERWIG 7.2.0 [66,67] for $Z \to ee/\tau\tau$ and $Z \to \mu\mu$, respectively. The simulation is accurate at NLO in QCD for up to two additional parton emissions and uses the MMHT2014$_{\text{NLO}}$ [68] set of PDFs.

Top quark pair production ($t\bar{t}$) was simulated at NLO in QCD using POWHEG BOX v2, and the h_{damp} parameter[5] set to 1.5 times the mass of the top quark [69]. The events were interfaced to PYTHIA 8.230 with the A14 set of tuning parameters and using the NNPDF2.3LO set of PDFs [70]. The shape of the $t\bar{t}$ background was corrected using a recursive generator-level reweighting to NNLO QCD plus NLO electroweak distributions, as described in Ref. [71]. This accounts for known mismodellings of some kinematic variables in the POWHEG BOX v2 $t\bar{t}$ simulation used here. The events were normalised to a cross section computed at NNLO in QCD with NNLL corrections [72–78].

Single top quark production in the s-channel and associated production of a top quark and W boson (Wt) were generated at NLO in QCD using POWHEG BOX v2 in the five-flavour scheme and using the NNPDF3.0$_{\text{NLO}}$ set of PDFs [79]. Single top quark production in the t-channel was generated at NLO in QCD using POWHEG BOX v2 in the four-flavour scheme. The diagram removal scheme [80] was used to remove diagrams that are modelled in both the tW and the $t\bar{t}$ MC samples. The events were normalised to a cross section computed at NLO in QCD with NNLL soft-gluon corrections [81,82].

The response of the detector for the above MC samples was modelled using a full simulation of the ATLAS detector [83] based on GEANT 4 [84]. Pile-up effects from the same and nearby bunch-crossings were modelled by overlaying minimum-bias hard-scatter events simulated using the soft QCD processes of PYTHIA 8.1 [85] with the A3 set of tuned parameters [86].

4. Object and event reconstruction

This analysis relies on selecting regions with enhanced purity in ggF and EW off-shell $H \to WW^*$ production based on the successful reconstruction of collision vertices, electrons, muons, jets, and the missing transverse momentum. Additionally, identification of jets containing b-hadrons (b-jets) is crucial to suppress top-quark-induced backgrounds. The definitions of these objects in the off-shell analysis are aligned with those of the on-shell $H \to WW^*$ analysis [22].

Vertices are reconstructed from tracks in the ID with transverse momentum $p_{\text{T}} > 500$ MeV, and events are required to have at least one vertex with at least two associated tracks. The primary vertex is selected as the vertex with the highest $\sum p_{\text{T}}^2$, where the sum is over all the tracks associated with that vertex.

Electron candidates are reconstructed by matching energy clusters in the EM calorimeter to well-reconstructed tracks that are extrapolated to the calorimeter [87]. Electron candidates are required to satisfy $|\eta| < 2.47$, excluding the transition region $1.37 < |\eta| < 1.52$ between the barrel and endcaps of the LAr calorimeter. Muon candidates are reconstructed from a global fit matching tracks from the inner detector and muon spectrometer [88]. They are required to satisfy $|\eta| < 2.5$. For both types of leptons, several additional requirements are made to reject particles misidentified as prompt leptons, including likelihood- and selection based identification criteria for electrons and muons, respectively. Electron candidates in events with less than two jets must satisfy the Tight likelihood working point criteria (70 % efficiency), and those in events with two jets or more must satisfy the Medium likelihood working point criteria (85 % efficiency) [89]. Muon candidates must satisfy the Tight identification working point criteria (95 % efficiency) [88]. The impact parameter requirements are $|z_0 \sin\theta| < 0.5$ mm and $|d_0|/\sigma_{d_0} < 5$ (3) for electrons (muons).[6] Lepton signatures are further required to be isolated from additional energy deposits and tracks in the event. The isolation requirement, defined using a multivariate method based on a boosted decision tree classifier, corresponds to the Tight working point of an improved algorithm relative to that used in Ref. [90]. This updated approach combines isolation variables with lifetime information derived from tracks in a jet reconstructed from the lepton's inner detector tracks, helping to distinguish prompt leptons from those originating in heavy-flavor decays. It achieves more than a factor of two improvement in rejecting misidentified leptons, while maintaining high efficiency for prompt leptons.

Jets are reconstructed using the anti-k_t algorithm with a radius parameter of $R = 0.4$ and particle flow objects as inputs [91–93]. Their four-momentum is corrected as explained in Ref. [94]. A jet-vertex-tagger multivariate discriminant selection that reduces contamination from pile-up [94] is applied to jets with $20 < p_{\text{T}} < 60$ GeV and $|\eta| < 2.4$; for jets with $|\eta| > 2.5$, a dedicated forward discriminant [95,96] is used. Jets are required to have $p_{\text{T}} > 20$ GeV and $|\eta| < 4.5$, but for the separation of events into jet multiplicity regions only jets with $p_{\text{T}} > 30$ GeV are counted. b-jets with $p_{\text{T}} > 20$ GeV and $|\eta| < 2.5$ are identified using a neural-network discriminant called DL1r [97]. This lower p_{T} requirement on the b-jets compared to jets is adopted to facilitate the definition of a 0-jet top control region. The working point that is adopted has an average 85 % b-jet tagging efficiency for simulated $t\bar{t}$ events. At the event selection stage, events are removed if they do not pass the jet cleaning criteria, which are designed to eliminate jets reconstructed from non-collision background processes [98]. Finally, standard kinematic and topological criteria are applied to the reconstructed leptons and jets to resolve overlaps, following the procedure outlined in Ref. [22].

The missing transverse momentum $\vec{p}_{\text{T}}^{\text{miss}}$, with magnitude $E_{\text{T}}^{\text{miss}}$, is calculated as the negative vector sum of the p_{T} of all the selected leptons and jets, together with reconstructed tracks that are not associated with these objects but are consistent with originating from the primary pp collision vertex and are referred to as the track soft term [99]. Missing

[5] The h_{damp} parameter is a resummation damping factor and one of the parameters that controls the matching of POWHEG matrix elements to the parton shower and thus effectively regulates the high-p_{T} radiation against which the $t\bar{t}$ system recoils.

[6] The transverse impact parameter, d_0, is defined by the point of closest approach of the track to the beamline in the $r-\phi$ plane. The longitudinal impact parameter, z_0, is the longitudinal distance to the hard-scatter primary vertex from this point. The uncertainty in the measurement of the transverse impact parameter is denoted by σ_{d_0}.

transverse momentum may also arise from the mismeasurement of the momentum of leptons or jets. The $E_{\mathrm{T}}^{\mathrm{miss}}$ significance, $\mathcal{S}(E_{\mathrm{T}}^{\mathrm{miss}})$, is used to mitigate this effect, and is calculated from the resolution of the physics objects used in the $E_{\mathrm{T}}^{\mathrm{miss}}$ reconstruction [99].

5. Event selection

A general preselection is first applied to all events for them to be considered in this analysis. Events are required to contain exactly two oppositely-charged leptons with $p_{\mathrm{T}} > 15\,\mathrm{GeV}$.[7] The leading lepton in the event is required to have $p_{\mathrm{T}} > 27\,\mathrm{GeV}$ and to be matched to the object that triggered the event. In the SF channel, events are also required to satisfy $p_{\mathrm{T}}^{\ell\ell} > 40\,\mathrm{GeV}$ and $\mathcal{S}(E_{\mathrm{T}}^{\mathrm{miss}}) > 4$, with $p_{\mathrm{T}}^{\ell\ell}$ defined as the magnitude of the transverse momentum of the di-lepton system.

The SF and DF channels are further split by jet multiplicity, separating events with 0, 1 and ≥ 2 jets. Additional event selections are applied in each of these jet multiplicity regions to define signal regions (SRs) and control regions (CRs), which are further detailed in the following sections.

5.1. Signal regions

The selections in the three DF SRs vary depending on the jet multiplicity. The invariant mass of the di-lepton system, $m_{\ell\ell}$, is required to be above 100 GeV, 80 GeV, and 70 GeV in the 0-jet, 1-jet, and ≥ 2-jets DF SRs, respectively. In the 0-jet DF SR, events with $55 \leq m_{\ell\ell} < 100\,\mathrm{GeV}$ are still selected if they satisfy $\Delta\phi_{(\ell,\ell)} > 2.0$. The $m_{\ell\ell}$ requirements both here and in the SF SRs ensure orthogonality with the on-shell $H \to WW^*$ analysis, which selects events with $m_{\ell\ell} < 55\,\mathrm{GeV}$ in the 0 and 1-jet multiplicity regions, and $m_{\ell\ell} < 70\,\mathrm{GeV}$ in the 2-jet multiplicity region [22]. Moreover, events in the 0-jet DF SR are required to satisfy $\Delta\eta_{(\ell,\ell)} < 1.8$, which cuts out a large proportion of $qq \to WW$ background events. Events in the 1-jet DF SR are required to satisfy $\Delta\phi_{(\ell,\ell)} > 1.8$, which facilitates the definition of an orthogonal 1-jet $qq \to WW$ CR while retaining most off-shell Higgs boson events in the SR. Events in all ≥ 2-jet SRs and CRs are required to satisfy the central jet veto (CJV) and outside lepton veto (OLV) requirements, which capitalize on the characteristic forward jets of the VBF process. The CJV ensures that the event does not contain a third jet within the pseudorapidity gap spanned by the two leading jets, reducing backgrounds from processes with QCD radiation, whereas the OLV requires that the leading leptons fall within this gap. Lastly, events in all SRs are required not to contain b-jets.

In the 0-jet and 1-jet SF SRs, $m_{\ell\ell}$ is required to be above 55 GeV, and in the 2-jet SF SR it is required to be above 70 GeV. In the 0-jet and 1-jet SF SRs, a selection of $\Delta\phi_{(\ell,\ell)} > 1.8$ is made, and this requirement ensures orthogonality with the on-shell $H \to WW^*$ analysis [22]. Events in all SF SRs are required to contain no b-jets, and must satisfy $|m_{\ell\ell} - 91\,\mathrm{GeV}| > 15\,\mathrm{GeV}$ to reject background processes containing Z bosons. The CJV and OLV are applied in the 2-jet SF SR. For a potential future combination, the events in all three SF SRs must satisfy $\Delta R_{(\ell,\ell)} > 1.8$. This selection ensures orthogonality with the $ZZ \to \ell\ell\nu\nu$ channel of the off-shell $H^* \to ZZ$ analysis [14], where the two leptons typically have a smaller angular separation as they originate from the same vector boson, in contrast to the $H^* \to WW$ channel.

5.2. Signal-background separation

DNN-based classifiers built with Tensorflow [100] are trained separately in each SR and are used to divide events into three DNN-score categories per SR, where the division was chosen to optimise expected analysis sensitivity. These DNNs are trained to separate both the full process (SBI) and the signal (S) from the non-interfering backgrounds listed in Section 6. For each SR, a subset of the following variables is provided as feature variables to the DNN: p_{T}, η, ϕ, and m of the leading and subleading lepton (ℓ_0 and ℓ_1)[8] and jets (j_0 and j_1); $p_{\mathrm{T}}^{\ell\ell}$; $|\Delta\eta_{(\ell,\ell)}|$; $|\Delta y_{(\ell,\ell)}|$; $|\Delta\phi_{(\ell,\ell)}|$; $\Delta R_{(\ell,\ell)}$; $m_{\ell\ell}$; m_{T}, the transverse mass, which is defined as $m_{\mathrm{T}} = \sqrt{(E_{\mathrm{T}}^{\ell\ell} + E_{\mathrm{T}}^{\mathrm{miss}})^2 - |\vec{p}_{\mathrm{T}}^{\,\ell\ell} + \vec{p}_{\mathrm{T}}^{\,\mathrm{miss}}|^2}$, where $E_{\ell\ell} = \sqrt{{p_{\mathrm{T}}^{\ell\ell}}^2 + m_{\ell\ell}^2}$; m_{jj}, the invariant mass of the two leading jets; $|\Delta y_{(j,j)}|$, computed from the two leading jets; $\sqrt{H_{\mathrm{T}}}$, where H_{T} is the sum of the scalar transverse momenta of preselected leptons and jets in the event; $\phi_{\vec{p}_{\mathrm{T}}^{\,\mathrm{miss}}}$; $\mathcal{S}(E_{\mathrm{T}}^{\mathrm{miss}})$; and $\Delta R_{(i,k)}$, where the ik combinations used are $\ell_0 j_0$, $\ell_0 j_1$ and $\ell_1 j_0$. In the 0-jet SR, a combination of variables associated to the leptons, $E_{\mathrm{T}}^{\mathrm{miss}}$ and event variables were chosen as DNN input variables. In the 1-jet and 2-jet SRs, permutation tests are used to select highly performing input variables. All of the MC predictions of DNNs and their input variables are consistent with data within the statistical and systematic uncertainties across all CRs described in Section 5.3.

In the training of the DNN, a simulated sample of W + jets events is used to model the contribution from misidentified lepton backgrounds. The training targets are ggF S and ggF SBI in the 0-jet regions, EW S and EW SBI in the 2-jet regions, and all of these contributions combined in the 1-jet regions. For both ggF and EW, the SBI and S processes are normalized equally in the SRs, ensuring that the model focuses also on S, which would otherwise contribute only minimally due to its relatively small yield. The combined sum of weights of all targets are scaled to equal the total sum of background weights in the training. This reweighting balances the otherwise very imbalanced classes, which aids in the training. Hyperparameter optimisations are performed separately for each DNN to maximise a significance-based sensitivity metric. A five-fold cross-validation[9] is used in the training and inference [101].

Due to the presence of destructive interference, the contributions to the event yields from the signal and interference may partially or completely cancel out, depending on the specific region of the phase space. However, they both contribute to the analysis sensitivity. As such, it is paramount to find a discriminant achieving high separation between signal and interference. The particle-level invariant mass of the WW system, m_{WW}, provides such separation to some extent, but due to the presence of the neutrinos in the final state, it is impossible to fully reconstruct m_{WW}. Instead, this analysis uses a linear combination of $m_{\ell\ell}$ and m_{T}, $V_{31} = 0.3 \cdot m_{\ell\ell} + 1 \cdot m_{\mathrm{T}}$, which provides a simple proxy for m_{WW}. The coefficient 0.3 and 1 were determined to be optimal in their m_{WW}-regression effectiveness by scanning for both a range of values between 0 and 1.

5.3. Control regions

The CRs are defined to estimate the normalisations of the leading background processes, and reduce the effect of systematic uncertainties by causing a partial cancellation of their impacts in the SRs. The selections that define all CRs are applied in addition to the DF pre-selection requirements; 1-jet CRs are defined for the $qq \to WW$ and $Z \to \tau\tau$ processes, and 0, 1 and ≥ 2-jet CRs are defined for the top quark backgrounds. For the $Z \to \tau\tau$ and $qq \to WW$ processes in SRs characterized by other jet multiplicities, and for the $Z \to \ell\ell$ process in all SRs, no corresponding CR is defined as the background-rich low DNN-score categories in the SRs provide sufficient constraining power.

[7] For the purpose of vetoing additional leptons at the preselection level, the identification and isolation criteria described in Section 4 are relaxed to the Medium and FixedCutLoose working points, respectively, for both muons and electrons.

[8] The lepton masses are not included.

[9] For each task, five independent DNNs are trained using a five-fold cross-validation strategy. The simulated events are split into five equal subsets; each DNN is trained on three, validated on one, and tested on the remaining subset. The roles of the subsets are rotated to ensure statistical independence between training, validation, and testing. Only the inference on the test subset, unused during training or validation, is used in the analysis

The $qq \to WW$ CR is required to contain no b-jets and to have $m_{\ell\ell}$ above 80 GeV. Events are also required to satisfy $\Delta\phi_{(\ell,\ell)} < 1.8$ as the $qq \to WW$ background exhibits a more uniform distribution compared to the ggF S process as a function of $\Delta\phi_{(\ell,\ell)}$, and $|m_{\tau\tau} - 91\,\text{GeV}| > 25\,\text{GeV}$, where $m_{\tau\tau}$ represents the assumed mass of the $\tau\tau$ system computed from the light leptons and $\vec{p}_{\text{T}}^{\text{miss}}$ under the collinear approximation.[10] Events for which this approximation yields no physical solution are also vetoed. The purity of $qq \to WW$ events in this CR is estimated to be 28 % using simulations.

The top quark CRs constrain the normalisation of the $t\bar{t}$ and Wt backgrounds. Events in the 0-jet and 1-jet (≥2-jet) CRs are required to have $m_{\ell\ell}$ above 100 GeV (70 GeV). In the 0-jet CR, there must be one b-jet with $20 < p_{\text{T}} < 30\,\text{GeV}$, and in the 1-jet and 2-jet CRs there must be exactly one b-jet with $p_{\text{T}} > 30\,\text{GeV}$. Events in the 0-jet CR are required to satisfy $\Delta\eta_{(\ell,\ell)} < 1.8$, and events in the 1-jet CR are required to satisfy $\Delta\phi_{(\ell,\ell)} > 1.8$. The 2-jet CR requires events to satisfy the CJV and OLV. The purity of top quark events is 93 % in the 0-jet top quark CR and 98 % in both the 1- and 2-jet top quark CRs as estimated using simulations.

Events in the $Z \to \tau\tau$ CR are required to satisfy $m_{\ell\ell} < 80\,\text{GeV}$ and not to contain any b-jets. Events in this CR are also required to have $m_{\tau\tau}$ larger than 66 GeV. The purity of $Z \to \tau\tau$ events in this CR is estimated to be 88 % using simulations.

6. Background estimation

This analysis is subject to two types of backgrounds: those that interfere with the signal and those that do not. The former were introduced in Section 1, while the latter include events from $qq \to WW$ processes, top-quark-induced backgrounds ($t\bar{t}$ and Wt), $Z \to \ell\ell$ and $Z \to \tau\tau$ decays, VVV events, WZ events, $V\gamma^*$ events, a tiny contribution from on-shell Higgs boson processes including $WH \to \ell\nu qq\ell\nu$, and events involving misidentified leptons. The normalisations of the $qq \to WW$, top-quark-induced, $Z \to \tau\tau$, and $Z \to \ell\ell$ backgrounds are estimated and constrained using data from the relevant CRs, described in Section 5, or low DNN-score categories in the SRs. Other background normalisations are derived from simulation except for the misidentified lepton background, which requires a dedicated data-driven approach.

The misidentified lepton background arises mainly from W + jets events, where jets are incorrectly identified as prompt leptons. The probability of such misidentification is small, but the large cross section of the W + jets process compared to that of the signal means that this background must still be taken into account. The normalisation and shape of this background are estimated using the data-driven fake-factor method [103], since it is not well modelled in simulation. This method uses an orthogonal misidentified-lepton-enriched control region, in which all nominal selections are applied except that at least one lepton candidate fails nominal lepton identification and isolation criteria but instead passes a looser set of criteria. The measured misidentified lepton background is estimated by subtracting the contribution from prompt background processes from data in the misidentified-lepton-enriched control region, and extrapolating to the SR using fake factors. These fake factors are evaluated as a function of p_{T} and $|\eta|$ in a region dominated by Z + jets events. The derivation of the fake factors is described in more detail in Ref. [22], in the context of the on-shell analysis.

7. Systematic uncertainties

The sensitivity of the analysis is impacted by several sources of systematic uncertainty that are related to the theoretical description of the simulated samples and the experimental uncertainties originating from the detector response.

Each analysis object defined in Section 4 has associated experimental uncertainties that are applied to the objects in MC simulations. For leptons, the uncertainties are related to the trigger, reconstruction, identification, and isolation selection efficiencies as well as the energy (or momentum) scale and resolution. For jets, uncertainties arise from the jet energy scale and resolution, the jet-vertex tagger performance, and the b-jet identification. Another source of uncertainty originates from the impact of the computation of the track soft term in the reconstruction of $\vec{p}_{\text{T}}^{\text{miss}}$. The uncertainty in the modelling of pile-up for simulated samples is estimated by varying the reweighting to the profile in data within its uncertainties. The uncertainty in the combined integrated luminosity is 0.83 % [32], obtained using the LUCID-2 detector [25] for the primary luminosity measurements.

The uncertainties in the misidentified lepton estimate, described in Section 6, have three main components: the statistical uncertainty in extrapolation factors derived in dedicated misidentified-lepton-enriched regions, the uncertainty from subtracting the simulated prompt lepton component, and the sample composition uncertainty detailed in Ref. [22]. The relative size of the uncertainty on the fake extrapolation factor depends on the lepton flavour and its momentum, and ranges roughly between 10 % and 70 %.

For all signal and major background processes, theory uncertainties related to the variation of the nominal choice of PDF, the QCD renormalisation and factorisation scales, and the strong coupling constant α_s are evaluated. For ggF B, ggF SBI, and ggF S, these uncertainties are derived on the NLO fixed-order prediction used to obtain the k-factors discussed in Section 3.2 and are correlated across all three samples.

For processes generated with SHERPA, uncertainties are evaluated in the choice of the matching scale between matrix element calculation and parton shower (CKKW [61]), the modelling of parton shower effects that include variation of the resummation scale (QSF), and the choice of parton shower recoil scheme (CSSKIN [60,62]). All three uncertainties are derived using particle-level samples.

Uncertainties in the parton shower simulation of EW SBI, EW SBI20, and EW B are estimated by comparing the expected yield from the corresponding simulated samples with that from alternative samples where the parton shower is simulated with HERWIG instead of PYTHIA. In addition, these samples include uncertainties in the modelling of the hard emissions and variations of the showering scale controlling the amount of radiation in both the initial and final states. Since these processes are only simulated at LO, an additional conservative constant 25 % uncertainty is applied to cover both electroweak and QCD NLO corrections [51].[11] A constant 20 % uncertainty is used for the remaining small contributions of on-shell ggF and VBF $H \to WW^*$ and a 50 % uncertainty for other minor Higgs boson production and decay modes.

For processes including top quarks, the NLO matching scheme uncertainty is applied and a comparison with the alternative generator HERWIG is used to cover differences in the showering and hadronisation schemes. In addition, uncertainties related to the modelling of initial- and final-state radiation are represented by varying scale, resummation, and showering parameters. The ordering choice in the 3D recursive reweighting is considered as an additional source of uncertainty for the $t\bar{t}$ process. For the Wt process, uncertainties related to the choice of h_{damp} scale [104] and diagram removal schemes [80] are applied.

The non-interfering single and diboson background SHERPA samples are affected by an uncertainty in the combination of the NLO QCD with NLO EW virtual approximate correction. An additional generator comparison uncertainty is assigned to cover an observed $p_T^{\ell\ell}$ shape mismodelling in the SHERPA 2.2.11/14 Z + jets processes [105]. For triboson processes, a constant 12 % theory uncertainty is used.

The systematic uncertainties alter the total number of expected events (normalisation) and shape of the V_{31} distributions. To remove

[10] The collinear approximation for $m_{\tau\tau}$ assumes the neutrinos travel in the same direction as the visible τ decay products, as detailed in Ref. [102].

[11] The k-factors in the paper provided are derived differentially and inclusively in a phase space that is not identical to the measured phase space in this analysis. Therefore, the size of the uncertainty was chosen as the largest correction provided in Ref. [51].

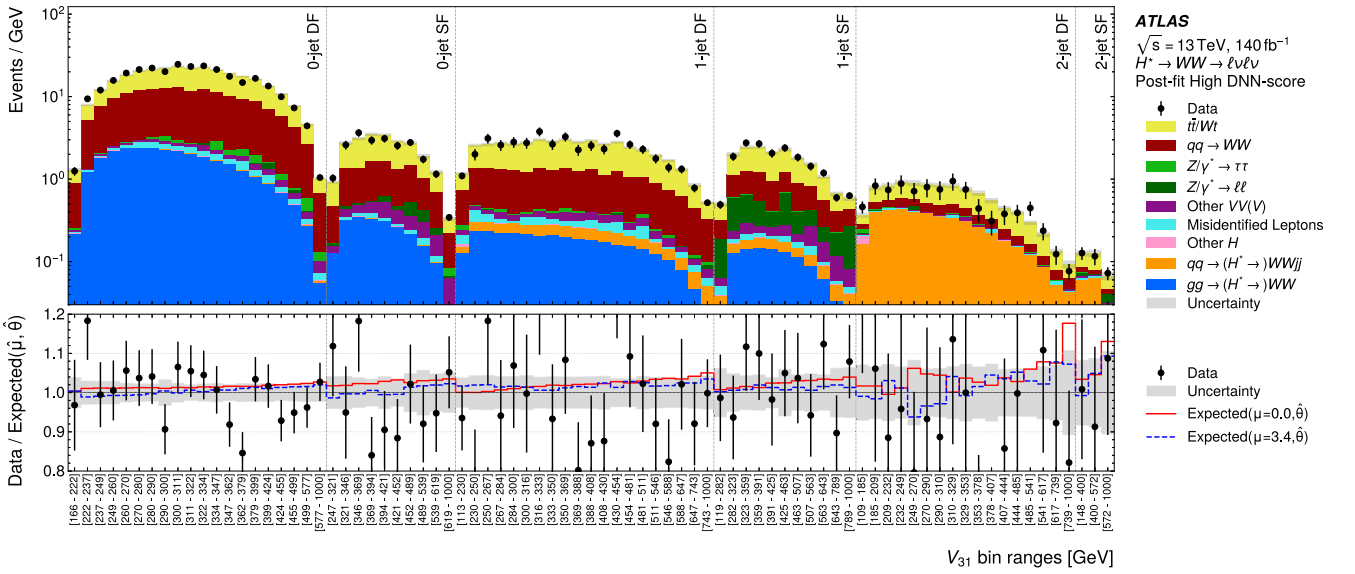

Fig. 2. Summary of the post-fit V_{31} distributions in the high DNN-score category of the SRs. The top panel shows the event yield divided by the bin width in each of the measured categories for both measured data (dots) and expected post-fit predictions (histograms). Overflow is included in the last bin of each distribution. The bottom panel shows the ratio of the data to the post-fit expected predictions. The sum in quadrature of statistical and systematic post-fit uncertainties are depicted by a grey band. Two alternative hypotheses are included, where the nuisance parameters are fixed to their best-fit values, $\hat{\theta}$, and the value of the parameter of interest $\mu_{\text{off-shell}} = 0$ (solid line) and $\mu_{\text{off-shell}} = 3.4$ (dashed line). The former represents the null hypothesis whereas the latter represents the upper bound of the symmetric 95 % CL interval of $\mu_{\text{off-shell}}$.

Table 1
Breakdown of the observed impact of sources of uncertainties on the value of $\mu_{\text{off-shell}}$ at 68 % confidence level where $t_{\mu_{\text{off-shell}}} = 1$. The values in the right column represent the relative difference in quadrature between the best-fit $\mu_{\text{off-shell}}$ and the $\mu_{\text{off-shell}}$ from a fit where a set of nuisance parameters (θ_i) are fixed to their best-fit values $\hat{\theta}_i$.

Statistical uncertainty	52 %
MC stat. uncertainty	15 %
Theory uncertainty	39 %
- Theory background	22 %
- Theory signal	34 %
Experimental uncertainty	25 %
- Jets	19 %
- Leptons	5.3 %
- Others	6.8 %
- Misidentified leptons	3.1 %
Background normalisation	7.6 %

negligible contributions and improve the stability of the fit, the systematics uncertainties are pruned, smoothed, and symmetrised. For the shape component of the uncertainties, only the theory uncertainties affecting $Z \to \ell\ell$, $Z \to \tau\tau$, ggF S, B, and SBI, as well as EW B, SBI, and SBI20 are retained, while all other shape uncertainties (from other sources or for other samples) are removed.

The systematic uncertainties described in this section are related to the off-shell signal strength measurement. When translating the signal strength in terms of the Higgs boson width, by combining with the on-shell results as described in Section 9, several systematic uncertainties (partially) cancel.

8. Statistical inference

To quantify the strength of the signal in the statistical model, the parameter of interest, μ, is measured in this analysis using the profile log-likelihood ratio [106] as test statistic:

$$t_\mu = -2\ln\frac{\lambda(\mu,\hat{\hat{\theta}})}{\lambda(\hat{\mu},\hat{\theta})}; \text{ which generalizes to } t_{\mu_1,\mu_2} = -2\ln\frac{\lambda(\mu_1,\mu_2,\hat{\hat{\theta}})}{\lambda(\hat{\mu}_1,\hat{\mu}_2,\hat{\theta})}$$

for cases with two parameters of interest, μ_1 and μ_2. Here, λ denotes the binned likelihood function, defined as the product of Poisson probability terms over all bins of V_{31} in the signal regions (SRs) and single-bin control regions (CRs) considered in the analysis, as introduced in Section 5. The likelihood function depends on the parameter(s) of interest and a set of nuisance parameters (NPs), θ, which account for systematic uncertainties discussed in Section 7. The maximum likelihood estimates of the parameters are denoted by $\hat{\mu}$ (equivalently $\hat{\mu}_1$ and $\hat{\mu}_2$) and $\hat{\theta}$, while $\hat{\hat{\theta}}$ represents the values of the nuisance parameters that maximize the likelihood function for a given μ (or equivalently μ_1 and μ_2).

The full ggF signal template, referred to as $\nu^{\text{ggF}}(\mu^{\text{ggF}}_{\text{off-shell}},\theta)$, for a given hypothesis $\mu_{\text{off-shell}}$ can be computed for each bin of the input distributions using the following parameterisation:

$$\begin{aligned}\nu^{\text{ggF}}(\mu^{\text{ggF}}_{\text{off-shell}},\theta) &= \mu^{\text{ggF}}_{\text{off-shell}}\cdot n^{\text{ggF}}_{\text{S}}(\theta) + \sqrt{\mu^{\text{ggF}}_{\text{off-shell}}}\cdot \\ &\quad \left(n^{\text{ggF}}_{\text{SBI}}(\theta) - n^{\text{ggF}}_{\text{S}}(\theta) - n^{\text{ggF}}_{\text{B}}(\theta)\right) + n^{\text{ggF}}_{\text{B}}(\theta) \\ &= \left(\mu^{\text{ggF}}_{\text{off-shell}} - \sqrt{\mu^{\text{ggF}}_{\text{off-shell}}}\right)\cdot n^{\text{ggF}}_{\text{S}}(\theta) + \sqrt{\mu^{\text{ggF}}_{\text{off-shell}}}\cdot n^{\text{ggF}}_{\text{SBI}}(\theta) \\ &\quad + \left(1 - \sqrt{\mu^{\text{ggF}}_{\text{off-shell}}}\right)\cdot n^{\text{ggF}}_{\text{B}}(\theta),\end{aligned}$$

where $n^{\text{ggF}}_{\text{S}}$, $n^{\text{ggF}}_{\text{B}}$ and $n^{\text{ggF}}_{\text{SBI}}$ represent the corresponding expected yields of the ggF S, ggF B, and ggF SBI processes, respectively. The interplay between signal and destructive interference leads to a non-monotonic total event yield as a function of $\mu_{\text{off-shell}}$. This can cause double minima in likelihood scans, a degeneracy that is lifted in part or fully by the information contained in the shape of the fitted V_{31} distributions. The definition of an off-shell signal-only template for the EW process is complicated by the presence of non-removable on-shell Higgs contributions as discussed in Section 3.2. Instead, the EW parameterisation uses n^{EW}_{B} and two $n^{\text{EW}}_{\text{SBI}}$ samples with $\mu^{\text{EW}}_{\text{off-shell}}$ scaled to 1 and 20 respectively. A detailed description of this parametrisation can be found in Table 1 of Ref. [14], where it was used in the $H \to ZZ$ channel.

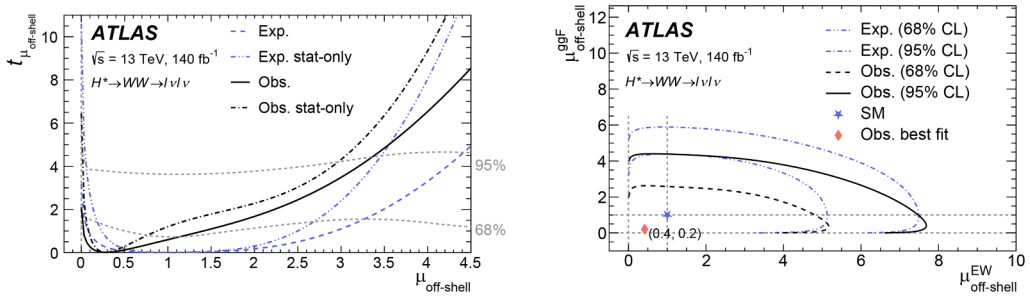

(a) (b)

Fig. 3. (a) Values of the test statistic $t_{\mu_{\text{off-shell}}}$ as a function of the off-shell Higgs boson signal strength, $\mu_{\text{off-shell}}$. The 68 % and 95 % CL are shown as gray dotted lines. (b) Contours of the values of the profile likelihood ratio $t_{\mu^{\text{ggF}}_{\text{off-shell}},\mu^{\text{EW}}_{\text{off-shell}}}$ as a function of $\mu^{\text{ggF}}_{\text{off-shell}}$ and $\mu^{\text{EW}}_{\text{off-shell}}$. The SM predicted value and best-fit value are indicated by a star and a diamond, respectively. The observed (expected) results are shown in black (blue) for scenarios with and without systematics. For (a) the 68 % and 95 % CL are calculated using an explicit Neyman construction, whereas in (b) they are calculated via the asymptotic approximation. (For interpretation of the references to color in this figure legend, the reader is referred to the web version of this article.)

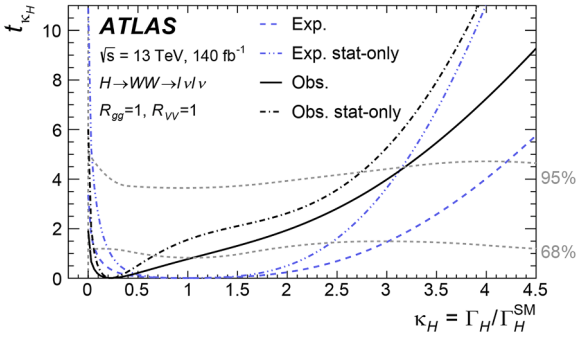

Fig. 4. Values of the test statistic t_{κ_H} as a function of $\kappa_H = \Gamma_H/\Gamma_H^{\text{SM}}$ for the combined on-shell and off-shell result assuming $R_{gg} = R_{VV} = 1$. The observed (expected) results are shown in black (blue) for scenarios with and without systematics. The 68 % and 95 % CL are shown as gray dotted lines. The 68 % and 95 % CL were calculated using an explicit Neyman construction. (For interpretation of the references to color in this figure legend, the reader is referred to the web version of this article.)

All experimental uncertainties, including those from misidentified leptons, are correlated across all measured analysis regions and categories. Theory uncertainties in ggF S, B, and SBI and separately in EW B, SBI, and SBI20 are also correlated across all analysis regions and categories whereas uncertainties in the non-interfering background are only correlated across lepton flavour channels but not across jet multiplicities. The exceptions are $V\gamma$, diboson processes (not including $qq \to WW$), and triboson processes which are also not correlated across lepton flavours due to the differences in the origin of the leptons in the final state across these channels.

The likelihood can be parameterised as a function of a single off-shell signal-strength parameter $\mu_{\text{off-shell}}$ that is applied to both Higgs boson production modes (ggF and EW), but alternatively two signal strength parameters for the ggF and EW process can be fully decorrelated and used separately: $\mu^{\text{ggF}}_{\text{off-shell}}$ and $\mu^{\text{EW}}_{\text{off-shell}}$.

The $\mu_{\text{off-shell}}$ measurement is combined with the measurement of $\mu_{\text{on-shell}}$ from Ref. [22] in a joint likelihood function. The result can be interpreted in terms of the width of the Higgs boson normalised to its SM expectation ($\mu_{\text{off-shell}}/\mu_{\text{on-shell}} = \Gamma_H/\Gamma_H^{\text{SM}} = \kappa_H$) or as the ratio of coupling modifiers in the off-shell and on-shell regimes ($R_{gg} = \kappa^2_{\text{g, off-shell}}/\kappa^2_{\text{g, on-shell}}$) and ($R_{VV} = \kappa^2_{\text{v, off-shell}}/\kappa^2_{\text{v, on-shell}}$). The κ_H interpretation assumes that the off- and on-shell coupling modifiers are the same for both ggF and EW production modes, while the R_{gg} and R_{VV} interpretations assume that the total width of the Higgs boson is equal to its SM prediction.

In the combination, nuisance parameters representing uncertainties from experimental sources and theory predictions in non-interfering backgrounds in the on- and off-shell analyses are correlated. The theory uncertainties in the interfering backgrounds are not correlated across the on- and off-shell phase spaces, as this would imply also correlating them with the uncertainties in the off-shell signal. The small contribution of on-shell signal in the off-shell analysis was correlated with the signal in the on-shell analysis. An extra selection is made in the on-shell $qq \to WW$ CR at $m_{\ell\ell} < 80$ GeV in the combination. This requirement removes the overlap between the $qq \to WW$ CRs in the 1-jet phase space of both analyses. Moreover, the $Z \to \tau\tau$ CR fully overlaps with the corresponding CR of the on-shell analysis. In the combination, an extra selection is therefore applied to the off-shell CR which requires $60 \le p_{\text{T}}^H < 120$ GeV, where p_{T}^H is defined as $\left|\vec{p}_{\text{T}}^{\,\ell\ell} + \vec{p}_{\text{T}}^{\,\text{miss}}\right|$. This fully aligns the CR definitions, creating a single CR that is shared between the two analyses.

9. Results

Using the likelihood function described in Section 8, a combined fit is performed on all analysis regions and categories. Fig. 2 shows the post-fit distributions for the V_{31} observable in the high DNN-score category of all signal regions.[12] Two alternate hypotheses are shown in the ratio pad at the bottom, representing the expected signal yield at $\mu_{\text{off-shell}} = 0$ and $\mu_{\text{off-shell}} = 3.4$, where it crosses the 95 % upper bound of the symmetric CL interval. In some bins both hypotheses vary in the same direction (up or down), reflecting the nonlinear parametrisation of the signal. The most sensitive regions are the 0-jet multiplicity regions due to the large event yields, followed by the 2-jet multiplicity regions due to their relatively high signal purities.

The values of the profile likelihood ratio as a function of $\mu_{\text{off-shell}}$ are shown in Fig. 3(a), both for the expected and for the observed results. Both of these also include the result with systematic uncertainties fixed to their best-fit values from a statistics-only fit, and the result where they are allowed to vary. The difference between the observed and expected values of the signal strength parameter $\mu_{\text{off-shell}}$ can be understood from degeneracies caused by the non-trivial (quadratic) dependence of the event yield as a function on $\mu_{\text{off-shell}}$. The quadratic dependence of signal and interference yields on $\mu_{\text{off-shell}}$ in the presence of over- or underfluctuations causes the distribution of the test statistic to depart from the asymptotic χ^2 distribution predicted by Wilks' theorem [107]. Therefore, the confidence intervals on $\mu_{\text{off-shell}}$ are constructed using the

[12] The binning optimisation of V_{31} is mostly driven by the requirement to have more than 1 and 10 signal and non-interfering background events per bin, respectively, and a relative statistical uncertainty below 20 % in each bin. In addition, the width of each bin is required to be above 10 GeV, and the maximum number of bins is imposed not to be larger than 20 in the high DNN-score categories to reduce the complexity of the fit. These criteria were varied to study the robustness of the binning and a minimal impact on the results was found.

Neyman construction [108]. These intervals are derived from the distribution of the profile likelihood ratio, evaluated for different values of the parameter of interest. The distribution is obtained through simulated pseudo-experiments, where event yields in each bin are sampled from the probability density function with nuisance parameters fixed to their best-fit values from data. The measurement yields observed (expected) central values and 68 % confidence level (CL) uncertainties on the signal strength of $\mu_{\text{off-shell}} = 0.3^{+0.9}_{-0.3}(1.0^{+2.3}_{-1.0})$. The observed (expected) upper bound on the measurement at 95 % CL on $\mu_{\text{off-shell}}$ is 3.4 (4.4). Table 7 shows the observed impact of groups of systematic uncertainties for the value of $\mu_{\text{off-shell}}$ at $t_{\mu_{\text{off-shell}}} = 1$ following the procedure described in Table 5 of Ref. [109]. The leading uncertainty is driven by the statistical precision of the available dataset, followed by theory and experimental uncertainties. In the $\mu_{\text{off-shell}}$ fit, all estimated background normalisations are compatible with the SM predictions within 95 % CL.

To probe the two off-shell signal strength parameters for the ggF and EW production modes, Fig. 3(b) shows the values of the profile likelihood ratio as a function of both $\mu^{\text{ggF}}_{\text{off-shell}}$ and $\mu^{\text{EW}}_{\text{off-shell}}$. The best-fit values for the parameters are observed (expected) to be $\mu^{\text{ggF}}_{\text{off-shell}} = 0.2^{+1.3}_{-0.2}$ $(1.0^{+2.5}_{-1.0})$ and $\mu^{\text{EW}}_{\text{off-shell}} = 0.4^{+3.4}_{-0.4}$ $(1.0^{+2.9}_{-1.0})$.

Higgs boson width measurement

As described in Section 8, the combination of this analysis with the on-shell $H \to WW^*$ analysis [22] allows for an interpretation in terms of the Higgs width normalized to its SM value, κ_H, or alternatively the ratio of the Higgs to gg and VV couplings squared in the on- and off-shell regimes, R_{gg} and R_{VV}. The resulting values of the test statistic t_{κ_H} are shown in Fig. 4 as a function of κ_H. Using $\Gamma^{\text{SM}}_H = 4.1$ MeV, the observed (expected) value for Γ_H is $0.9^{+3.4}_{-0.9}$ $(4.1^{+8.3}_{-3.8}$ MeV) and the observed (expected) upper bound at 95 % confidence level on Γ_H is 13.1 (17.3) MeV. The interpretation in terms of R_{VV} yields an observed (expected) value of $0.6^{+1.6}_{-0.6}$ $(1.0^{+1.2}_{-1.0})$, while the R_{gg} interpretation is not sufficiently sensitive to set upper bounds at 68 % as the likelihood function rapidly flattens. In all interpretations, the estimated background normalisations are compatible with those from the $\mu_{\text{off-shell}}$ fit within 68 % CL.

10. Conclusion

This Letter describes an analysis of off-shell production of Higgs bosons in the $H \to WW^*$ channel, using leptonic final states and performed on the $\sqrt{s} = 13$ TeV pp collision data-set collected with the ATLAS detector during Run 2 of the LHC. No significant deviation from the Standard Model expectation is observed. The data are used to constrain the signal strength for off-shell Higgs boson production, yielding an observed (expected) measurement of $\mu_{\text{off-shell}}$ at $0.3^{+0.9}_{-0.3}$ $(1.0^{+2.3}_{-1.0})$ with an upper bound of 3.4 (4.4) at 95 % CL. This is a significant improvement over the ATLAS LHC Run 1 measurement of $\mu_{\text{off-shell}}$ in the $H \to WW^*$ channel, which found an observed (expected) upper limit of 17.2 (21.3) at 95 % CL [17].

This analysis is combined with a measurement of on-shell Higgs boson production in the $H \to WW^*$ channel, and the results of the combination are interpreted as a constraint on the Higgs boson total width. Under the assumption that the off- and on-shell coupling modifiers are the same for both ggF and EW production modes, the observed (expected) value for Γ_H is $0.9^{+3.4}_{-0.9}$ $(4.1^{+8.3}_{-3.8})$ MeV, where the Standard Model predicts a value of 4.1 MeV [6]. An observed (expected) upper bound at 95 % confidence level on the Higgs boson total width is measured at 13.1 (17.3) MeV.

Data availability

The data for this manuscript are not available. The values in the plots and tables associated to this article are stored in HEPDATA (https://www.hepdata.net/record/157579/).

Declaration of competing interest

The authors declare that they have no known competing financial interests or personal relationships that could have appeared to influence the work reported in this paper.

Acknowledgement

We thank CERN for the very successful operation of the LHC and its injectors, as well as the support staff at CERN and at our institutions worldwide without whom ATLAS could not be operated efficiently.

The crucial computing support from all WLCG partners is acknowledged gratefully, in particular from CERN, the ATLAS Tier-1 facilities at TRIUMF/SFU (Canada), NDGF (Denmark, Norway, Sweden), CC-IN2P3 (France), KIT/GridKA (Germany), INFN-CNAF (Italy), NL-T1 (Netherlands), PIC (Spain), RAL (UK) and BNL (USA), the Tier-2 facilities worldwide and large non-WLCG resource providers. Major contributors of computing resources are listed in Ref. [110].

We gratefully acknowledge the support of ANPCyT, Argentina; YerPhI, Armenia; ARC, Australia; BMWFW and FWF, Austria; ANAS, Azerbaijan; CNPq and FAPESP, Brazil; NSERC, NRC and CFI, Canada; CERN; ANID, Chile; CAS, MOST and NSFC, China; Minciencias, Colombia; MEYS CR, Czech Republic; DNRF and DNSRC, Denmark; IN2P3-CNRS and CEA-DRF/IRFU, France; SRNSFG, Georgia; BMFTR, HGF and MPG, Germany; GSRI, Greece; RGC and Hong Kong SAR, China; ICHEP and Academy of Sciences and Humanities, Israel; INFN, Italy; MEXT and JSPS, Japan; CNRST, Morocco; NWO, Netherlands; RCN, Norway; MNiSW, Poland; FCT, Portugal; MNE/IFA, Romania; MSTDI, Serbia; MSSR, Slovakia; ARIS and MVZI, Slovenia; DSI/NRF, South Africa; MICIU/AEI, Spain; SRC and Wallenberg Foundation, Sweden; SERI, SNSF and Cantons of Bern and Geneva, Switzerland; NSTC, Taipei; TENMAK, Türkiye; STFC/UKRI, United Kingdom; DOE and NSF, United States of America.

Individual groups and members have received support from BCKDF, CANARIE, CRC and DRAC, Canada; CERN-CZ, FORTE and PRIMUS, Czech Republic; COST, ERC, ERDF, Horizon 2020, ICSC-NextGenerationEU and Marie Skłodowska-Curie Actions, European Union; Investissements d'Avenir Labex, Investissements d'Avenir Idex and ANR, France; DFG and AvH Foundation, Germany; Herakleitos, Thales and Aristeia programmes co-financed by EU-ESF and the Greek NSRF, Greece; BSF-NSF and MINERVA, Israel; NCN and NAWA, Poland; La Caixa Banking Foundation, CERCA Programme Generalitat de Catalunya and PROMETEO and GenT Programmes Generalitat Valenciana, Spain; Göran Gustafssons Stiftelse, Sweden; The Royal Society and Leverhulme Trust, United Kingdom.

In addition, individual members wish to acknowledge support from Armenia: Yerevan Physics Institute (FAPERJ); CERN: European Organization for Nuclear Research (CERN DOCT); Chile: Agencia Nacional de Investigación y Desarrollo (FONDECYT 1230812, FONDECYT 1240864); China: Chinese Ministry of Science and Technology (MOST-2023YFA1605700, MOST-2023YFA1609300), National Natural Science Foundation of China (NSFC - 12175119, NSFC 12275265); Czech Republic: Czech Science Foundation (GACR - 24-11373S), Ministry of Education Youth and Sports (ERC-CZ-LL2327, FORTE CZ.02.01.01/00/22_008/0004632), PRIMUS Research Programme (PRIMUS/21/SCI/017); EU: H2020 European Research Council (ERC - 101002463); European Union: European Research Council (BARD No. 101116429, ERC - 948254, ERC 101089007), European Regional Development Fund (SMASH COFUND 101081355, SLO ERDF), Horizon 2020 Framework Programme (MUCCA - CHIST-ERA-19-XAI-00), European Union, Future Artificial Intelligence Research (FAIR-NextGenerationEU PE00000013), Horizon 2020 (EuroHPC - EHPC-DEV-2024D11-051), Italian Center for High Performance Computing, Big Data and Quantum Computing (ICSC, NextGenerationEU); France: Agence Nationale de la Recherche (ANR-21-CE31-0022, ANR-22-EDIR-0002); Germany: Baden-Württemberg Stiftung (BW Stiftung-Postdoc Eliteprogramme),

Deutsche Forschungsgemeinschaft (DFG - 469666862, DFG - CR 312/5-2); China: Research Grants Council (GRF); Italy: Istituto Nazionale di Fisica Nucleare (ICSC, NextGenerationEU), Ministero dell'Università e della Ricerca (NextGenEU 153D23001490006 M4C2.1.1, NextGenEU I53D23000820006 M4C2.1.1, NextGenEU I53D23001490006 M4C2.1.1); Japan: Japan Society for the Promotion of Science (JSPS KAKENHI JP22H01227, JSPS KAKENHI JP22H04944, JSPS KAKENHI JP22KK0227, JSPS KAKENHI JP23KK0245, JSPS KAKENHI JP24K23939); Norway: Research Council of Norway (RCN-314472); Poland: Ministry of Science and Higher Education (IDUB AGH, POB8, D4 no 9722), Polish National Science Centre (NCN 2021/42/E/ST2/00350, NCN OPUS 2023/51/B/ST2/02507, NCN OPUS nr 2022/47/B/ST2/03059, NCN UMO-2019/34/E/ST2/00393, UMO-2022/47/O/ST2/00148, UMO-2023/49/B/ST2/04085, UMO-2023/51/B/ST2/00920, UMO-2024/53/N/ST2/00869); Portugal: Foundation for Science and Technology (FCT); Spain: Generalitat Valenciana (Artemisa, FEDER, IDIFEDER/2018/048), Ministry of Science and Innovation (MCIN & NextGenEU PCI2022-135018-2, MICIN & FEDER PID2021-125273NB, RYC2019-028510-I, RYC2020-030254-I, RYC2021-031273-I, RYC2022-038164-I); Sweden: Carl Trygger Foundation (Carl Trygger Foundation CTS 22:2312), Swedish Research Council (Swedish Research Council 2023-04654, VR 2021-03651, VR 2022-03845, VR 2022-04683, VR 2023-03403, VR 2024-05451), Knut and Alice Wallenberg Foundation (KAW 2018.0458, KAW 2022.0358, KAW 2023.0366); Switzerland: Swiss National Science Foundation (SNSF - PCEFP2_194658); United Kingdom: Leverhulme Trust (Leverhulme Trust RPG-2020-004), Royal Society (NIF-R1-231091); United States of America: U.S. Department of Energy (ECA DE-AC02-76SF00515), Neubauer Family Foundation.

The ATLAS Collaboration

G. Aad[104], E. Aakvaag[17], B. Abbott[123], S. Abdelhameed[119a], K. Abeling[55], N.J. Abicht[49], S.H. Abidi[30], M. Aboelela[45], A. Aboulhorma[36e], H. Abramowicz[157], Y. Abulaiti[120], B.S. Acharya[69a,69b,n], A. Ackermann[63a], C. Adam Bourdarios[4], L. Adamczyk[87a], S.V. Addepalli[149], M.J. Addison[103], J. Adelman[118], A. Adiguzel[22c], T. Adye[137], A.A. Affolder[139], Y. Afik[40], M.N. Agaras[13], A. Aggarwal[102], C. Agheorghiesei[28c], F. Ahmadov[39,ae], S. Ahuja[97], X. Ai[143b], G. Aielli[76a,76b], A. Aikot[169], M. Ait Tamlihat[36e], B. Aitbenchikh[36a], M. Akbiyik[102], T.P.A. Åkesson[100], A.V. Akimov[151], D. Akiyama[174], N.N. Akolkar[25], S. Aktas[22a], G.L. Alberghi[24b], J. Albert[171], P. Albicocco[53], G.L. Albouy[60], S. Alderweireldt[52], Z.L. Alegria[124], M. Aleksa[37], I.N. Aleksandrov[39], C. Alexa[28b], T. Alexopoulos[10], F. Alfonsi[24b], M. Algren[56], M. Alhroob[173], B. Ali[135], H.M.J. Ali[93,x], S. Ali[32], S.W. Alibocus[94], M. Aliev[34c], G. Alimonti[71a], W. Alkakhi[55], C. Allaire[66], B.M.M. Allbrooke[152], J.S. Allen[103], J.F. Allen[52], P.P. Allport[21], A. Aloisio[72a,72b], F. Alonso[92], C. Alpigiani[142], Z.M.K. Alsolami[93], A. Alvarez Fernandez[102], M. Alves Cardoso[56], M.G. Alviggi[72a,72b], M. Aly[103], Y. Amaral Coutinho[83b], A. Ambler[106], C. Amelung[37], M. Amerl[103], C.G. Ames[111], T. Amezza[130], D. Amidei[108], B. Amini[54], K. Amirie[161], A. Amirkhanov[39], S.P. Amor Dos Santos[133a], K.R. Amos[169], D. Amperiadou[158], S. An[84], C. Anastopoulos[145], T. Andeen[11], J.K. Anders[94], A.C. Anderson[59], A. Andreazza[71a,71b], S. Angelidakis[9], A. Angerami[42], A.V. Anisenkov[39], A. Annovi[74a], C. Antel[56], E. Antipov[151], M. Antonelli[53], F. Anulli[75a], M. Aoki[84], T. Aoki[159], M.A. Aparo[152], L. Aperio Bella[48], M. Apicella[31], C. Appelt[157], A. Apyan[27], S.J. Arbiol Val[88], C. Arcangeletti[53], A.T.H. Arce[51], J-F. Arguin[110], S. Argyropoulos[158], J.-H. Arling[48], O. Arnaez[4], H. Arnold[151], G. Artoni[75a,75b], H. Asada[113], K. Asai[121], S. Asai[159], S. Asatryan[179], N.A. Asbah[37], R.A. Ashby Pickering[173], A.M. Aslam[97], K. Assamagan[30], R. Astalos[29a], K.S.V. Astrand[100], S. Atashi[165], R.J. Atkin[34a], H. Atmani[36f], P.A. Atmasiddha[131], K. Augsten[135], A.D. Auriol[41], V.A. Austrup[103], G. Avolio[37], K. Axiotis[56], G. Azuelos[110,ai], D. Babal[29b], H. Bachacou[138], K. Bachas[158,r], A. Bachiu[35], E. Bachmann[50], M.J. Backes[63a], A. Badea[40], T.M. Baer[108], P. Bagnaia[75a,75b], M. Bahmani[19], D. Bahner[54], K. Bai[126], J.T. Baines[137], L. Baines[96], O.K. Baker[178], E. Bakos[16], D. Bakshi Gupta[8], L.E. Balabram Filho[83b], V. Balakrishnan[123], R. Balasubramanian[4], E.M. Baldin[38], P. Balek[87a], E. Ballabene[24b,24a], F. Balli[138], L.M. Baltes[63a], W.K. Balunas[33], J. Balz[102], I. Bamwidhi[119b], E. Banas[88], M. Bandieramonte[132], A. Bandyopadhyay[25], S. Bansal[25], L. Barak[157], M. Barakat[48], E.L. Barberio[107], D. Barberis[18b], M. Barbero[104], M.Z. Barel[117], T. Barillari[112], M-S. Barisits[37], T. Barklow[149], P. Baron[136], D.A. Baron Moreno[103], A. Baroncelli[62], A.J. Barr[129], J.D. Barr[98], F. Barreiro[101], J. Barreiro Guimarães da Costa[14], M.G. Barros Teixeira[133a], S. Barsov[38], F. Bartels[63a], R. Bartoldus[149], A.E. Barton[93], P. Bartos[29a], A. Basan[102], M. Baselga[49], S. Bashiri[88], A. Bassalat[66,b], M.J. Basso[162a], S. Bataju[45], R. Bate[170], R.L. Bates[59], S. Batlamous[101], M. Battaglia[139], D. Battulga[19], M. Bauce[75a,75b], M. Bauer[79], P. Bauer[25], L.T. Bayer[48], L.T. Bazzano Hurrell[31], J.B. Beacham[112], T. Beau[130], J.Y. Beaucamp[92], P.H. Beauchemin[164], P. Bechtle[25], H.P. Beck[20,q], K. Becker[173], A.J. Beddall[82], V.A. Bednyakov[39], C.P. Bee[151], L.J. Beemster[16], M. Begalli[83d], M. Begel[30], J.K. Behr[48], J.F. Beirer[37], F. Beisiegel[25], M. Belfkir[119b], G. Bella[157], L. Bellagamba[24b], A. Bellerive[35], C.D. Bellgraph[68], P. Bellos[21], K. Beloborodov[38], D. Benchekroun[36a], F. Bendebba[36a], Y. Benhammou[157], K.C. Benkendorfer[61], L. Beresford[48], M. Beretta[53], E. Bergeaas Kuutmann[167], N. Berger[4], B. Bergmann[135], J. Beringer[18a], G. Bernardi[5], C. Bernius[149], F.U. Bernlochner[25], F. Bernon[37], A. Berrocal Guardia[13], T. Berry[97], P. Berta[136], A. Berthold[50], A. Berti[133a], R. Bertrand[104], S. Bethke[112], A. Betti[75a,75b], A.J. Bevan[96], L. Bezio[56], N.K. Bhalla[54], S. Bharthuar[112], S. Bhatta[151], P. Bhattarai[149], Z.M. Bhatti[120], K.D. Bhide[54], V.S. Bhopatkar[124], R.M. Bianchi[132], G. Bianco[24b,24a], O. Biebel[111], M. Biglietti[77a], C.S. Billingsley[45], Y. Bimgdi[36f], M. Bindi[55], A. Bingham[177], A. Bingul[22b], C. Bini[75a,75b], G.A. Bird[33], M. Birman[175], M. Biros[136], S. Biryukov[152], T. Bisanz[49], E. Bisceglie[24b,24a], J.P. Biswal[137], D. Biswas[147], I. Bloch[48], A. Blue[59], U. Blumenschein[96], J. Blumenthal[102], V.S. Bobrovnikov[39], L. Boccardo[57b,57a], M. Boehler[54], B. Boehm[172], D. Bogavac[13], A.G. Bogdanchikov[38], L.S. Boggia[130], V. Boisvert[97], P. Bokan[37], T. Bold[87a], M. Bomben[5], M. Bona[96], M. Boonekamp[138], A.G. Borbély[59], I.S. Bordulev[38], G. Borissov[93], D. Bortoletto[129], D. Boscherini[24b], M. Bosman[13], K. Bouaouda[36a], N. Bouchhar[169], L. Boudet[4], J. Boudreau[132], E.V. Bouhova-Thacker[93], D. Boumediene[41], R. Bouquet[57b,57a], A. Boveia[122], J. Boyd[37], D. Boye[30], I.R. Boyko[39], L. Bozianu[56], J. Bracinik[21], N. Brahimi[4], G. Brandt[177], O. Brandt[33], B. Brau[105], J.E. Brau[126], R. Brener[175], L. Brenner[117], R. Brenner[167], S. Bressler[175], G. Brianti[78a,78b], D. Britton[59], D. Britzger[112], I. Brock[25], R. Brock[109], G. Brooijmans[42], A.J. Brooks[68], E.M. Brooks[162b], E. Brost[30], L.M. Brown[171,162a], L.E. Bruce[61], T.L. Bruckler[129], P.A. Bruckman de Renstrom[88], B. Brüers[48], A. Bruni[24b], G. Bruni[24b], D. Brunner[47a,47b], M. Bruschi[24b], N. Bruscino[75a,75b], T. Buanes[17], Q. Buat[142], D. Buchin[112], A.G. Buckley[59], O. Bulekov[82], B.A. Bullard[149], S. Burdin[94], C.D. Burgard[49], A.M. Burger[91], B. Burghgrave[8], O. Burlayenko[54], J. Burleson[168], J.C. Burzynski[148], E.L. Busch[42], V. Büscher[102], P.J. Bussey[59], J.M. Butler[26], C.M. Buttar[59], J.M. Butterworth[98], W. Buttinger[137], C.J. Buxo Vazquez[109], A.R. Buzykaev[39], S. Cabrera Urbán[169], L. Cadamuro[66], D. Caforio[58], H. Cai[132], Y. Cai[24b,114c,24a], Y. Cai[114a], V.M.M. Cairo[37], O. Cakir[3a], N. Calace[37], P. Calafiura[18a], G. Calderini[130], P. Calfayan[35], G. Callea[59], L.P. Caloba[83b], D. Calvet[41], S. Calvet[41], R. Camacho Toro[130], S. Camarda[37], D. Camarero Munoz[27], P. Camarri[76a,76b], C. Camincher[171], M. Campanelli[98],

A. Camplani[43], V. Canale[72a,72b], A.C. Canbay[3a], E. Canonero[97], J. Cantero[169], Y. Cao[168], F. Capocasa[27], M. Capua[44b,44a], A. Carbone[71a,71b], R. Cardarelli[76a], J.C.J. Cardenas[8], M.P. Cardiff[27], G. Carducci[44b,44a], T. Carli[37], G. Carlino[72a], J.I. Carlotto[13], B.T. Carlson[132,s], E.M. Carlson[171], J. Carmignani[94], L. Carminati[71a,71b], A. Carnelli[4], M. Carnesale[37], S. Caron[116], E. Carquin[140f], I.B. Carr[107], S. Carrá[73a,73b], G. Carratta[24b,24a], A.M. Carroll[126], M.P. Casado[13,i], P. Casolaro[72a,72b], M. Caspar[48], F.L. Castillo[4], L. Castillo Garcia[13], V. Castillo Gimenez[169], N.F. Castro[133a,133e], A. Catinaccio[37], J.R. Catmore[128], T. Cavaliere[4], V. Cavaliere[30], L.J. Caviedes Betancourt[23b], E. Celebi[82], S. Cella[37], V. Cepaitis[56], K. Cerny[125], A.S. Cerqueira[83a], A. Cerri[74a,74b,al], L. Cerrito[76a,76b], F. Cerutti[18a], B. Cervato[71a,71b], A. Cervelli[24b], G. Cesarini[53], S.A. Cetin[82], P.M. Chabrillat[130], R. Chakkappai[66], S. Chakraborty[173], J. Chan[18a], W.Y. Chan[159], J.D. Chapman[33], E. Chapon[138], B. Chargeishvili[155b], D.G. Charlton[21], C. Chauhan[136], Y. Che[114a], S. Chekanov[6], S.V. Chekulaev[162a], G.A. Chelkov[39,a], B. Chen[157], B. Chen[171], H. Chen[114a], H. Chen[30], J. Chen[144a], J. Chen[148], M. Chen[129], S. Chen[89], S.J. Chen[114a], X. Chen[144a], X. Chen[15,ah], Z. Chen[62], C.L. Cheng[176], H.C. Cheng[64a], S. Cheong[149], A. Cheplakov[39], E. Cherepanova[117], R. Cherkaoui El Moursli[36e], E. Cheu[7], K. Cheung[65], L. Chevalier[138], V. Chiarella[53], G. Chiarelli[74a], G. Chiodini[70a], A.S. Chisholm[21], A. Chitan[28b], M. Chitishvili[169], M.V. Chizhov[39,t], K. Choi[11], Y. Chou[142], E.Y.S. Chow[116], K.L. Chu[175], M.C. Chu[64a], X. Chu[14,114c], Z. Chubinidze[53], J. Chudoba[134], J.J. Chwastowski[88], D. Cieri[112], K.M. Ciesla[87a], V. Cindro[95], A. Ciocio[18a], F. Cirotto[72a,72b], Z.H. Citron[175], M. Citterio[71a], D.A. Ciubotaru[28b], A. Clark[56], P.J. Clark[52], N. Clarke Hall[98], C. Clarry[161], S.E. Clawson[48], C. Clement[47a,47b], Y. Coadou[104], M. Cobal[69a,69c], A. Coccaro[57b], R.F. Coelho Barrue[133a], R. Coelho Lopes De Sa[105], S. Coelli[71a], L.S. Colangeli[161], B. Cole[42], P. Collado Soto[101], J. Collot[60], R. Coluccia[70a,70b], P. Conde Muiño[133a,133g], M.P. Connell[34c], S.H. Connell[34c], E.I. Conroy[129], M. Contreras Cossio[11], F. Conventi[72a,aj], H.G. Cooke[21], A.M. Cooper-Sarkar[129], L. Corazzina[75a,75b], F.A. Corchia[24b,24a], A. Cordeiro Oudot Choi[142], L.D. Corpe[41], M. Corradi[75a,75b], F. Corriveau[106,ac], A. Cortes-Gonzalez[159], M.J. Costa[169], F. Costanza[4], D. Costanzo[145], B.M. Cote[122], J. Couthures[4], G. Cowan[97], K. Cranmer[176], L. Cremer[49], D. Cremonini[24b,24a], S. Crépé-Renaudin[60], F. Crescioli[130], T. Cresta[73a,73b], M. Cristinziani[147], M. Cristoforetti[78a,78b], V. Croft[117], J.E. Crosby[124], G. Crosetti[44b,44a], A. Cueto[101], H. Cui[98], Z. Cui[7], W.R. Cunningham[59], F. Curcio[169], J.R. Curran[52], M.J. Da Cunha Sargedas De Sousa[57b,57a], J.V. Da Fonseca Pinto[83b], C. Da Via[103], W. Dabrowski[87a], T. Dado[37], S. Dahbi[154], T. Dai[108], D. Dal Santo[20], C. Dallapiccola[105], M. Dam[43], G. D'amen[30], V. D'Amico[111], J. Damp[102], J.R. Dandoy[35], D. Dannheim[37], G. D'anniballe[74a,74b], M. Danninger[148], V. Dao[151], G. Darbo[57b], S.J. Das[30], F. Dattola[48], S. D'Auria[71a,71b], A. D'Avanzo[72a,72b], T. Davidek[136], J. Davidson[173], I. Dawson[96], K. De[8], C. De Almeida Rossi[161], R. De Asmundis[72a], N. De Biase[48], S. De Castro[24b,24a], N. De Groot[116], P. de Jong[117], H. De la Torre[118], A. De Maria[114a], A. De Salvo[75a], U. De Sanctis[76a,76b], F. De Santis[70a,70b], A. De Santo[152], J.B. De Vivie De Regie[60], J. Debevc[95], D.V. Dedovich[39], J. Degens[94], A.M. Deiana[45], J. Del Peso[101], L. Delagrange[130], F. Deliot[138], C.M. Delitzsch[49], M. Della Pietra[72a,72b], D. Della Volpe[56], A. Dell'Acqua[37], L. Dell'Asta[71a,71b], M. Delmastro[4], C.C. Delogu[102], P.A. Delsart[60], S. Demers[178], M. Demichev[39], S.P. Denisov[38], H. Denizli[22a,m], L. D'Eramo[41], D. Derendarz[88], F. Derue[130], P. Dervan[94], A.M. Desai[1], K. Desch[25], F.A. Di Bello[57b,57a], A. Di Ciaccio[76a,76b], L. Di Ciaccio[4], A. Di Domenico[75a,75b], C. Di Donato[72a,72b], A. Di Girolamo[37], G. Di Gregorio[37], A. Di Luca[78a,78b], B. Di Micco[77a,77b], R. Di Nardo[77a,77b], K.F. Di Petrillo[40], M. Diamantopoulou[35], F.A. Dias[117], M.A. Diaz[140a,140b], A.R. Didenko[39], M. Didenko[169], S.D. Diefenbacher[18a], E.B. Diehl[108], S. Díez Cornell[48], C. Diez Pardos[147], C. Dimitriadi[150], A. Dimitrievska[21], A. Dimri[151], J. Dingfelder[25], T. Dingley[129], I-M. Dinu[28b], S.J. Dittmeier[63b], F. Dittus[37], M. Divisek[136], B. Dixit[94], F. Djama[104], T. Djobava[155b], C. Doglioni[103,100], A. Dohnalova[29a], Z. Dolezal[136], K. Domijan[87a], K.M. Dona[40], M. Donadelli[83d], B. Dong[109], J. Donini[41], A. D'Onofrio[72a,72b], M. D'Onofrio[94], J. Dopke[137], A. Doria[72a], N. Dos Santos Fernandes[133a], P. Dougan[103], M.T. Dova[92], A.T. Doyle[59], M.A. Draguet[129], M.P. Drescher[55], E. Dreyer[175], I. Drivas-koulouris[10], M. Drnevich[120], M. Drozdova[56], D. Du[62], T.A. du Pree[117], Z. Duan[114a], M. Dubau[4], F. Dubinin[39], M. Dubovsky[29a], E. Duchovni[175], G. Duckeck[111], P.K. Duckett[98], O.A. Ducu[28b], D. Duda[52], A. Dudarev[37], E.R. Duden[27], M. D'uffizi[103], L. Duflot[66], M. Dührssen[37], I. Duminica[28g], A.E. Dumitriu[28b], M. Dunford[63a], S. Dungs[49], K. Dunne[47a,47b], A. Duperrin[104], H. Duran Yildiz[3a], M. Düren[58], A. Durglishvili[155b], D. Duvnjak[35], G.I. Dyckes[18a], M. Dyndal[87a], B.S. Dziedzic[37], Z.O. Earnshaw[152], G.H. Eberwein[129], B. Eckerova[29a], S. Eggebrecht[55], E. Egidio Purcino De Souza[83e], G. Eigen[17], K. Einsweiler[18a], T. Ekelof[167], P.A. Ekman[100], S. El Farkh[36b], Y. El Ghazali[62], H. El Jarrari[37], A. El Moussaouy[36a], V. Ellajosyula[167], M. Ellert[167], F. Ellinghaus[177], N. Ellis[37], J. Elmsheuser[30], M. Elsawy[119a], M. Elsing[37], D. Emeliyanov[137], Y. Enari[84], I. Ene[18a], S. Epari[110], D. Ernani Martins Neto[88], F. Ernst[37], M. Errenst[177], M. Escalier[66], C. Escobar[169], E. Etzion[157], G. Evans[133a,133b], H. Evans[68], L.S. Evans[97], A. Ezhilov[38], S. Ezzarqtouni[36a], F. Fabbri[24b,24a], L. Fabbri[24b,24a], G. Facini[98], V. Fadeyev[139], R.M. Fakhrutdinov[38], D. Fakoudis[102], S. Falciano[75a], L.F. Falda Ulhoa Coelho[133a], F. Fallavollita[112], G. Falsetti[44b,44a], J. Faltova[136], C. Fan[168], K.Y. Fan[64b], Y. Fan[14], Y. Fang[14,114c], M. Fanti[71a,71b], M. Faraj[69a,69b], Z. Farazpay[99], A. Farbin[8], A. Farilla[77a], T. Farooque[109], J.N. Farr[178], S.M. Farrington[137,52], F. Fassi[36e], D. Fassouliotis[9], L. Fayard[66], P. Federic[136], P. Federicova[134], O.L. Fedin[38,a], M. Feickert[176], L. Feligioni[104], D.E. Fellers[18a], C. Feng[143a], Z. Feng[117], M.J. Fenton[165], L. Ferencz[48], B. Fernandez Barbadillo[93], P. Fernandez Martinez[67], M.J.V. Fernoux[104], J. Ferrando[93], A. Ferrari[167], P. Ferrari[117,116], R. Ferrari[73a], D. Ferrere[56], C. Ferretti[108], M.P. Fewell[1], D. Fiacco[75a,75b], F. Fiedler[102], P. Fiedler[135], S. Filimonov[39], M.S. Filip[28b,u], A. Filipčič[95], E.K. Filmer[162a], F. Filthaut[116], M.C.N. Fiolhais[133a,133c,c], L. Fiorini[169], W.C. Fisher[109], T. Fitschen[103], P.M. Fitzhugh[138], I. Fleck[147], P. Fleischmann[108], T. Flick[177], M. Flores[34d,ag], L.R. Flores Castillo[64a], L. Flores Sanz De Acedo[37], F.M. Follega[78a,78b], N. Fomin[33], J.H. Foo[161], A. Formica[138], A.C. Forti[103], E. Fortin[37], A.W. Fortman[18a], L. Foster[18a], L. Fountas[9,j], D. Fournier[66], H. Fox[93], P. Francavilla[74a,74b], S. Francescato[61], S. Franchellucci[56], M. Franchini[24b,24a], S. Franchino[63a], D. Francis[37], L. Franco[116], V. Franco Lima[37], L. Franconi[48], M. Franklin[61], G. Frattari[27], Y.Y. Frid[157], J. Friend[59], N. Fritzsche[37], A. Froch[56], D. Froidevaux[37], J.A. Frost[129], Y. Fu[109], S. Fuenzalida Garrido[140f], M. Fujimoto[104], K.Y. Fung[64a], E. Furtado De Simas Filho[83e], M. Furukawa[159], J. Fuster[169], A. Gaa[55], A. Gabrielli[24b,24a], A. Gabrielli[161], P. Gadow[37], G. Gagliardi[57b,57a], L.G. Gagnon[18a], S. Gaid[85b], S. Galantzan[157], J. Gallagher[1], E.J. Gallas[129], A.L. Gallen[167], B.J. Gallop[137], K.K. Gan[122], S. Ganguly[159], Y. Gao[52], A. Garabaglu[142], F.M. Garay Walls[140a,140b], C. García[169], A. Garcia Alonso[117], A.G. Garcia Caffaro[178], J.E. García Navarro[169], M. Garcia-Sciveres[18a], G.L. Gardner[131], R.W. Gardner[40], N. Garelli[164], R.B. Garg[149], J.M. Gargan[52], C.A. Garner[161], C.M. Garvey[34a], V.K. Gassmann[164], G. Gaudio[73a], V. Gautam[13], P. Gauzzi[75a,75b], J. Gavranovic[95], I.L. Gavrilenko[133a], A. Gavrilyuk[38], C. Gay[170], G. Gaycken[126], E.N. Gazis[10], A. Gekow[122], C. Gemme[57b], M.H. Genest[60], A.D. Gentry[115], S. George[97], T. Geralis[46], A.A. Gerwin[123], P. Gessinger-Befurt[37],

M.E. Geyik[177], M. Ghani[173], K. Ghorbanian[96], A. Ghosal[147], A. Ghosh[165], A. Ghosh[7], B. Giacobbe[24b], S. Giagu[75a,75b], T. Giani[117], A. Giannini[62], S.M. Gibson[97], M. Gignac[139], D.T. Gil[87b], A.K. Gilbert[87a], B.J. Gilbert[42], D. Gillberg[35], G. Gilles[117], D.M. Gingrich[2,ai], M.P. Giordani[69a,69c], P.F. Giraud[138], G. Giugliarelli[69a,69c], D. Giugni[71a], F. Giuli[76a,76b], I. Gkialas[9,j], L.K. Gladilin[38], C. Glasman[101], M. Glazewska[20], R.M. Gleason[165], G. Glemža[48], M. Glisic[126], I. Gnesi[44b], Y. Go[30], M. Goblirsch-Kolb[37], B. Gocke[49], D. Godin[110], B. Gokturk[22a], S. Goldfarb[107], T. Golling[56], M.G.D. Gololo[34c], D. Golubkov[38], J.P. Gombas[109], A. Gomes[133a,133b], G. Gomes Da Silva[147], A.J. Gomez Delegido[169], R. Gonçalo[133a], L. Gonella[21], A. Gongadze[155c], F. Gonnella[21], J.L. Gonski[149], R.Y. González Andana[52], S. González de la Hoz[169], M.V. Gonzalez Rodrigues[48], R. Gonzalez Suarez[167], S. Gonzalez-Sevilla[56], L. Goossens[37], B. Gorini[37], E. Gorini[70a,70b], A. Gorišek[95], T.C. Gosart[131], A.T. Goshaw[51], M.I. Gostkin[39], S. Goswami[124], C.A. Gottardo[37], S.A. Gotz[111], M. Gouighri[36b], A.G. Goussiou[142], N. Govender[34c], R.P. Grabarczyk[129], I. Grabowska-Bold[87a], K. Graham[35], E. Gramstad[128], S. Grancagnolo[70a,70b], C.M. Grant[1], P.M. Gravila[28f], F.G. Gravili[70a,70b], H.M. Gray[18a], M. Greco[112], M.J. Green[1], C. Grefe[25], A.S. Grefsrud[17], I.M. Gregor[48], K.T. Greif[165], P. Grenier[149], S.G. Grewe[112], A.A. Grillo[139], K. Grimm[32], S. Grinstein[13,y], J.-F. Grivaz[66], E. Gross[175], J. Grosse-Knetter[55], L. Guan[108], G. Guerrieri[37], R. Guevara[128], R. Gugel[102], J.A.M. Guhit[108], A. Guida[19], E. Guilloton[173], S. Guindon[37], F. Guo[14,114c], J. Guo[144a], L. Guo[48], L. Guo[114b,w], Y. Guo[108], A. Gupta[49], R. Gupta[132], S. Gupta[27], S. Gurbuz[25], S.S. Gurdasani[48], G. Gustavino[75a,75b], P. Gutierrez[123], L.F. Gutierrez Zagazeta[131], M. Gutsche[50], C. Gutschow[98], C. Gwenlan[129], C.B. Gwilliam[94], E.S. Haaland[128], A. Haas[120], M. Habedank[59], C. Haber[18a], H.K. Hadavand[8], A. Haddad[41], A. Hadef[50], A.I. Hagan[93], J.J. Hahn[147], E.H. Haines[98], M. Haleem[172], J. Haley[124], G.D. Hallewell[104], L. Halser[20], K. Hamano[171], M. Hamer[25], S.E.D. Hammoud[66], E.J. Hampshire[97], J. Han[143a], L. Han[114a], L. Han[62], S. Han[18a], K. Hanagaki[84], M. Hance[139], D.A. Hangal[42], H. Hanif[148], M.D. Hank[131], J.B. Hansen[43], P.H. Hansen[43], D. Harada[56], T. Harenberg[177], S. Harkusha[179], M.L. Harris[105], Y.T. Harris[25], J. Harrison[13], N.M. Harrison[122], P.F. Harrison[173], M.L.E. Hart[98], N.M. Hartman[112], N.M. Hartmann[111], R.Z. Hasan[97,137], Y. Hasegawa[146], F. Haslbeck[129], S. Hassan[17], R. Hauser[109], M. Haviernik[136], C.M. Hawkes[21], R.J. Hawkings[37], Y. Hayashi[159], D. Hayden[109], C. Hayes[108], R.L. Hayes[117], C.P. Hays[129], J.M. Hays[96], H.S. Hayward[94], M. He[14,114c], Y. He[48], Y. He[98], N.B. Heatley[96], V. Hedberg[100], C. Heidegger[54], K.K. Heidegger[54], J. Heilman[35], S. Heim[48], T. Heim[18a], J.G. Heinlein[131], J.J. Heinrich[126], L. Heinrich[112], J. Hejbal[134], M. Helbig[50], A. Held[176], S. Hellesund[17], C.M. Helling[170], S. Hellman[47a,47b], A.M. Henriques Correia[37], H. Herde[100], Y. Hernández Jiménez[151], L.M. Herrmann[25], T. Herrmann[50], G. Herten[54], R. Hertenberger[111], L. Hervas[37], M.E. Hesping[102], N.P. Hessey[162a], J. Hessler[112], M. Hidaoui[36b], N. Hidic[136], E. Hill[161], T.S. Hillersoy[17], S.J. Hillier[21], J.R. Hinds[109], F. Hinterkeuser[25], M. Hirose[127], S. Hirose[163], D. Hirschbuehl[177], T.G. Hitchings[103], B. Hiti[95], J. Hobbs[151], R. Hobincu[28e], N. Hod[175], A.M. Hodges[168], M.C. Hodgkinson[145], B.H. Hodkinson[129], A. Hoecker[37], D.D. Hofer[108], J. Hofer[169], M. Holzbock[37], L.B.A.H. Hommels[33], V. Homsak[129], B.P. Honan[103], J.J. Hong[68], T.M. Hong[132], B.H. Hooberman[168], W.H. Hopkins[6], M.C. Hoppesch[168], Y. Horii[113], M.E. Horstmann[112], S. Hou[154], M.R. Housenga[168], A.S. Howard[95], J. Howarth[59], J. Hoya[6], M. Hrabovsky[125], T. Hryn'ova[4], P.J. Hsu[65], S.-C. Hsu[142], T. Hsu[66], M. Hu[18a], Q. Hu[62], S. Huang[33], X. Huang[14,114c], Y. Huang[136], Y. Huang[114b], Y. Huang[102], Y. Huang[14], Z. Huang[66], Z. Hubacek[135], M. Huebner[25], F. Huegging[25], T.B. Huffman[129], M. Hufnagel Maranha De Faria[83a], C.A. Hugli[48], M. Huhtinen[37], S.K. Huiberts[17], R. Hulsken[106], C.E. Hultquist[18a], N. Huseynov[12,g], J. Huston[109], J. Huth[61], R. Hyneman[7], G. Iacobucci[56], G. Iakovidis[30], L. Iconomidou-Fayard[66], J.P. Iddon[37], P. Iengo[72a,72b], R. Iguchi[159], Y. Iiyama[159], T. Iizawa[159], Y. Ikegami[84], D. Iliadis[158], N. Ilic[161], H. Imam[36a], G. Inacio Goncalves[83d], S.A. Infante Cabanas[140c], T. Ingebretsen Carlson[47a,47b], J.M. Inglis[96], G. Introzzi[73a,73b], M. Iodice[77a], V. Ippolito[75a,75b], R.K. Irwin[94], M. Ishino[159], W. Islam[176], C. Issever[19], S. Istin[22a,an], K. Itabashi[84], H. Ito[174], R. Iuppa[78a,78b], A. Ivina[175], V. Izzo[72a], P. Jacka[134], P. Jackson[1], P. Jain[48], K. Jakobs[54], T. Jakoubek[175], J. Jamieson[59], W. Jang[159], S. Jankovych[136], M. Javurkova[105], P. Jawahar[103], L. Jeanty[126], J. Jejelava[155a,af], P. Jenni[54,f], C.E. Jessiman[35], C. Jia[143a], H. Jia[170], J. Jia[151], X. Jia[14,114c], Z. Jia[114a], C. Jiang[52], Q. Jiang[64b], S. Jiggins[48], M. Jimenez Ortega[169], J. Jimenez Pena[13], S. Jin[114a], A. Jinaru[28b], O. Jinnouchi[141], P. Johansson[145], K.A. Johns[7], J.W. Johnson[139], F.A. Jolly[48], D.M. Jones[152], E. Jones[48], K.S. Jones[8], P. Jones[33], R.W.L. Jones[93], T.J. Jones[94], H.L. Joos[55,37], R. Joshi[122], J. Jovicevic[16], X. Ju[18a], J.J. Junggeburth[37], T. Junkermann[63a], A. Juste Rozas[13,y], M.K. Juzek[88], S. Kabana[140e], A. Kaczmarska[88], M. Kado[112], H. Kagan[122], M. Kagan[149], A. Kahn[131], C. Kahra[102], T. Kaji[159], E. Kajomovitz[156], N. Kakati[175], N. Kakoty[13], I. Kalaitzidou[54], S. Kandel[8], N.J. Kang[139], D. Kar[34g], K. Karava[129], E. Karentzos[25], O. Karkout[117], S.N. Karpov[39], Z.M. Karpova[39], V. Kartvelishvili[93], A.N. Karyukhin[38], E. Kasimi[158], J. Katzy[48], S. Kaur[35], K. Kawade[146], M.P. Kawale[123], C. Kawamoto[89], T. Kawamoto[62], E.F. Kay[37], F.I. Kaya[164], S. Kazakos[109], V.F. Kazanin[38], J.M. Keaveney[34a], R. Keeler[171], G.V. Kehris[61], J.S. Keller[35], J.J. Kempster[152], O. Kepka[134], J. Kerr[162b], B.P. Kerridge[137], B.P. Kerševan[95], L. Keszeghova[29a], R.A. Khan[132], A. Khanov[124], A.G. Kharlamov[38], T. Kharlamova[38], E.E. Khoda[142], M. Kholodenko[133a], T.J. Khoo[19], G. Khoriauli[172], Y. Khoulaki[36a], J. Khubua[155b,*], Y.A.R. Khwaira[130], B. Kibirige[34g], D. Kim[6], D.W. Kim[47a,47b], Y.K. Kim[40], N. Kimura[98], M.K. Kingston[55], A. Kirchhoff[55], C. Kirfel[25], F. Kirfel[25], J. Kirk[137], A.E. Kiryunin[112], S. Kita[163], O. Kivernyk[25], M. Klassen[164], C. Klein[35], L. Klein[172], M.H. Klein[45], S.B. Klein[56], U. Klein[94], A. Klimentov[30], T. Klioutchnikova[37], P. Kluit[117], S. Kluth[112], E. Kneringer[79], T.M. Knight[161], A. Knue[49], M. Kobel[50], D. Kobylianskii[175], S.F. Koch[129], M. Kocian[149], P. Kodyš[136], D.M. Koeck[126], T. Koffas[35], O. Kolay[50], I. Koletsou[4], T. Komarek[88], K. Köneke[55], A.X.Y. Kong[1], T. Kono[121], N. Konstantinidis[98], P. Kontaxakis[56], B. Konya[100], R. Kopeliansky[42], S. Koperny[87a], K. Korcyl[88], K. Kordas[158,d], A. Korn[98], S. Korn[55], I. Korolkov[13], N. Korotkova[38], B. Kortman[117], O. Kortner[112], S. Kortner[112], W.H. Kostecka[118], M. Kostov[29a], V.V. Kostyukhin[147], A. Kotsokechagia[37], A. Kotwal[51], A. Koulouris[37], A. Kourkoumeli-Charalampidi[73a,73b], C. Kourkoumelis[9], E. Kourlitis[112], O. Kovanda[126], R. Kowalewski[171], W. Kozanecki[126], A.S. Kozhin[38], V.A. Kramarenko[38], G. Kramberger[95], P. Kramer[25], M.W. Krasny[130], A. Krasznahorkay[105], A.C. Kraus[118], J.W. Kraus[177], J.A. Kremer[48], N.B. Krengel[147], T. Kresse[50], L. Kretschmann[177], J. Kretzschmar[94], K. Kreul[19], P. Krieger[161], K. Krizka[21], K. Kroeninger[49], H. Kroha[112], J. Kroll[134], J. Kroll[131], K.S. Krowpman[109], U. Kruchonak[39], H. Krüger[25], N. Krumnack[81], M.C. Kruse[51], O. Kuchinskaia[39], S. Kuday[3a], S. Kuehn[37], R. Kuesters[54], T. Kuhl[48], V. Kukhtin[39], Y. Kulchitsky[39], S. Kuleshov[140d,140b], J. Kull[1], E.V. Kumar[111], M. Kumar[34g], N. Kumari[48], P. Kumari[162b], A. Kupco[134], T. Kupfer[49], A. Kupich[38], O. Kuprash[54], H. Kurashige[86], L.L. Kurchaninov[162a], O. Kurdysh[4], Y.A. Kurochkin[38], A. Kurova[38], M. Kuze[141], A.K. Kvam[105], J. Kvita[125], N.G. Kyriacou[108], C. Lacasta[169], F. Lacava[75a,75b], H. Lacker[19], D. Lacour[130], N.N. Lad[98], E. Ladygin[39], A. Lafarge[41], B. Laforge[130], T. Lagouri[178], F.Z. Lahbabi[36a], S. Lai[55], J.E. Lambert[171], S. Lammers[68], W. Lampl[7],

C. Lampoudis[158,d], G. Lamprinoudis[102], A.N. Lancaster[118], E. Lançon[30], U. Landgraf[54], M.P.J. Landon[96], V.S. Lang[54], O.K.B. Langrekken[128], A.J. Lankford[165], F. Lanni[37], K. Lantzsch[25], A. Lanza[73a], M. Lanzac Berrocal[169], J.F. Laporte[138], T. Lari[71a], D. Larsen[17], L. Larson[11], F. Lasagni Manghi[24b], M. Lassnig[37], S.D. Lawlor[145], R. Lazaridou[173], M. Lazzaroni[71a,71b], H.D.M. Le[109], E.M. Le Boulicaut[178], L.T. Le Pottier[18a], B. Leban[24b,24a], F. Ledroit-Guillon[60], T.F. Lee[162b], L.L. Leeuw[34c], M. Lefebvre[171], C. Leggett[18a], G. Lehmann Miotto[37], M. Leigh[56], W.A. Leight[105], W. Leinonen[116], A. Leisos[158,v], M.A.L. Leite[83c], C.E. Leitgeb[19], R. Leitner[136], K.J.C. Leney[45], T. Lenz[25], S. Leone[74a], C. Leonidopoulos[52], A. Leopold[150], J.H. Lepage Bourbonnais[35], R. Les[109], C.G. Lester[33], M. Levchenko[38], J. Levêque[4], L.J. Levinson[175], G. Levrini[24b,24a], M.P. Lewicki[88], C. Lewis[142], D.J. Lewis[4], L. Lewitt[145], A. Li[30], B. Li[143a], C. Li[108], C-Q. Li[112], H. Li[143a], H. Li[103], H. Li[15], H. Li[62], H. Li[143a], J. Li[144a], K. Li[14], L. Li[144a], R. Li[178], S. Li[14,114c], S. Li[144b,144a], T. Li[5], X. Li[106], Z. Li[159], Z. Li[14,114c], Z. Li[62], S. Liang[14,114c], Z. Liang[14], M. Liberatore[138], B. Liberti[76a], K. Lie[64c], J. Lieber Marin[83e], H. Lien[68], H. Lin[108], S.F. Lin[151], L. Linden[111], R.E. Lindley[7], J.H. Lindon[37], J. Ling[61], E. Lipeles[131], A. Lipniacka[17], A. Lister[170], J.D. Little[68], B. Liu[14], B.X. Liu[114b], D. Liu[144b,144a], D. Liu[139], E.H.L. Liu[21], J.K.K. Liu[120], K. Liu[144b], K. Liu[144b,144a], M. Liu[62], M.Y. Liu[62], P. Liu[14], Q. Liu[144b,142,144a], X. Liu[62], X. Liu[143a], Y. Liu[114b,114c], Y.L. Liu[143a], Y.W. Liu[62], Z. Liu[66,l], S.L. Lloyd[96], E.M. Lobodzinska[48], P. Loch[7], E. Lodhi[161], T. Lohse[19], K. Lohwasser[145], E. Loiacono[48], J.D. Lomas[21], J.D. Long[42], I. Longarini[165], R. Longo[168], A. Lopez Solis[13], N.A. Lopez-canelas[7], N. Lorenzo Martinez[4], A.M. Lory[111], M. Losada[119a], G. Löschcke Centeno[152], X. Lou[47a,47b], X. Lou[14,114c], A. Lounis[66], P.A. Love[93], M. Lu[66], S. Lu[131], Y.J. Lu[154], H.J. Lubatti[142], C. Luci[75a,75b], F.L. Lucio Alves[114a], F. Luehring[68], B.S. Lunday[131], O. Lundberg[150], J. Lunde[37], N.A. Luongo[6], M.S. Lutz[37], A.B. Lux[26], D. Lynn[30], R. Lysak[134], V. Lysenko[135], E. Lytken[100], V. Lyubushkin[39], T. Lyubushkina[39], M.M. Lyukova[151], M.Firdaus M. Soberi[52], H. Ma[30], K. Ma[62], L.L. Ma[143a], W. Ma[62], Y. Ma[124], J.C. MacDonald[102], P.C. Machado De Abreu Farias[83e], R. Madar[41], T. Madula[98], J. Maeda[86], T. Maeno[30], P.T. Mafa[34c,k], H. Maguire[145], V. Maiboroda[66], A. Maio[133a,133b,133d], K. Maj[87a], O. Majersky[48], S. Majewski[126], R. Makhmanazarov[38], N. Makovec[66], V. Maksimovic[16], B. Malaescu[130], J. Malamant[128], Pa. Malecki[88], V.P. Maleev[38], F. Malek[60,p], M. Mali[95], D. Malito[97], U. Mallik[80,*], A. Maloizel[5], S. Maltezos[10], A. Malvezzi Lopes[83d], S. Malyukov[39], J. Mamuzic[13], G. Mancini[53], M.N. Mancini[27], G. Manco[73a,73b], J.P. Mandalia[96], S.S. Mandarry[152], I. Mandić[95], L. Manhaes de Andrade Filho[83a], I.M. Maniatis[175], J. Manjarres Ramos[91], D.C. Mankad[175], A. Mann[111], T. Manoussos[37], M.N. Mantinan[40], S. Manzoni[37], L. Mao[144a], X. Mapekula[34c], A. Marantis[158], R.R. Marcelo Gregorio[96], G. Marchiori[5], M. Marcisovsky[134], C. Marcon[71a], E. Maricic[16], M. Marinescu[48], S. Marium[48], M. Marjanovic[123], A. Markhoos[54], M. Markovitch[66], M.K. Maroun[105], G.T. Marsden[103], E.J. Marshall[93], Z. Marshall[18a], S. Marti-Garcia[169], J. Martin[98], T.A. Martin[137], V.J. Martin[52], B. Martin dit Latour[17], L. Martinelli[75a,75b], M. Martinez[13,y], P. Martinez Agullo[169], V.I. Martinez Outschoorn[105], P. Martinez Suarez[13], S. Martin-Haugh[137], G. Martinovicova[136], V.S. Martoiu[28b], A.C. Martyniuk[98], A. Marzin[37], D. Mascione[78a,78b], L. Masetti[102], J. Masik[103], A.L. Maslennikov[39], S.L. Mason[42], P. Massarotti[72a,72b], P. Mastrandrea[74a,74b], A. Mastroberardino[44b,44a], T. Masubuchi[127], T.T. Mathew[126], J. Matousek[136], D.M. Mattern[49], J. Maurer[28b], T. Maurin[59], A.J. Maury[66], B. Maček[95], C. Mavungu Tsava[104], D.A. Maximov[38], A.E. May[103], E. Mayer[41], R. Mazini[34g], I. Maznas[118], S.M. Mazza[139], E. Mazzeo[37], J.P. Mc Gowan[171], S.P. Mc Kee[108], C.A. Mc Lean[6], C.C. McCracken[170], E.F. McDonald[107], A.E. McDougall[117], L.F. Mcelhinney[93], J.A. Mcfayden[152], R.P. McGovern[131], R.P. Mckenzie[34g], T.C. Mclachlan[48], D.J. Mclaughlin[98], S.J. McMahon[137], C.M. Mcpartland[94], R.A. McPherson[171,ac], S. Mehlhase[111], A. Mehta[94], D. Melini[169], B.R. Mellado Garcia[34g], A.H. Melo[55], F. Meloni[48], A.M. Mendes Jacques Da Costa[103], L. Meng[93], S. Menke[112], M. Mentink[37], E. Meoni[44b,44a], G. Mercado[118], S. Merianos[158], C. Merlassino[69a,69c], C. Meroni[71a,71b], J. Metcalfe[6], A.S. Mete[6], E. Meuser[102], C. Meyer[68], J-P. Meyer[138], Y. Miao[114a], R.P. Middleton[137], M. Mihovilovic[66], L. Mijović[52], G. Mikenberg[175], M. Mikestikova[134], M. Mikuž[95], H. Mildner[102], A. Milic[37], D.W. Miller[40], E.H. Miller[149], L.S. Miller[35], A. Milov[175], D.A. Milstead[47a,47b], T. Min[114a], A.A. Minaenko[38], I.A. Minashvili[155b], A.I. Mincer[120], B. Mindur[87a], M. Mineev[39], Y. Mino[89], L.M. Mir[13], M. Miralles Lopez[59], M. Mironova[18a], M. Missio[116], A. Mitra[173], V.A. Mitsou[169], Y. Mitsumori[113], O. Miu[161], P.S. Miyagawa[96], T. Mkrtchyan[63a], M. Mlinarevic[98], T. Mlinarevic[98], M. Mlynarikova[37], S. Mobius[20], M.H. Mohamed Farook[115], S. Mohapatra[42], S. Mohiuddin[124], G. Mokgatitswane[34g], L. Moleri[175], U. Molinatti[129], L.G. Mollier[20], B. Mondal[134], S. Mondal[135], K. Mönig[48], E. Monnier[104], L. Monsonis Romero[169], J. Montejo Berlingen[13], A. Montella[47a,47b], M. Montella[122], F. Montereali[77a,77b], F. Monticelli[92], S. Monzani[69a,69c], A. Morancho Tarda[43], N. Morange[66], A.L. Moreira De Carvalho[48], M. Moreno Llácer[169], C. Moreno Martinez[56], J.M. Moreno Perez[23b], P. Morettini[57b], S. Morgenstern[37], M. Morii[61], M. Morinaga[159], M. Moritsu[90], F. Morodei[75a,75b], P. Moschovakos[37], B. Moser[54], M. Mosidze[155b], T. Moskalets[45], P. Moskvitina[116], J. Moss[32], P. Moszkowicz[87a], A. Moussa[36d], Y. Moyal[175], H. Moyano Gomez[13], E.J.W. Moyse[105], O. Mtintsilana[34g], S. Muanza[104], M. Mucha[25], J. Mueller[132], R. Müller[37], G.A. Mullier[167], A.J. Mullin[33], J.J. Mullin[51], A.C. Mullins[45], A.E. Mulski[61], D.P. Mungo[161], D. Munoz Perez[169], F.J. Munoz Sanchez[103], W.J. Murray[173,137], M. Muškinja[95], C. Mwewa[48], A.G. Myagkov[38,a], A.J. Myers[8], G. Myers[108], M. Myska[135], B.P. Nachman[18a], K. Nagai[129], K. Nagano[84], R. Nagasaka[159], J.L. Nagle[30,ak], E. Nagy[104], A.M. Nairz[37], Y. Nakahama[84], K. Nakamura[84], K. Nakkalil[5], A. Nandi[63b], H. Nanjo[127], E.A. Narayanan[45], Y. Narukawa[159], I. Naryshkin[38], L. Nasella[71a,71b], S. Nasri[119b], C. Nass[25], G. Navarro[23a], J. Navarro-Gonzalez[169], A. Nayaz[19], P.Y. Nechaeva[38], S. Nechaeva[24b,24a], F. Nechansky[134], L. Nedic[129], T.J. Neep[21], A. Negri[73a,73b], M. Negrini[24b], C. Nellist[117], C. Nelson[106], K. Nelson[108], S. Nemecek[134], M. Nessi[37,h], M.S. Neubauer[168], J. Newell[94], P.R. Newman[21], Y.W.Y. Ng[168], B. Ngair[119a], H.D.N. Nguyen[110], J.D. Nichols[123], R.B. Nickerson[129], R. Nicolaidou[138], J. Nielsen[139], M. Niemeyer[55], J. Niermann[37], N. Nikiforou[37], V. Nikolaenko[38,a], I. Nikolic-Audit[130], P. Nilsson[30], I. Ninca[48], G. Ninio[157], A. Nisati[75a], N. Nishu[2], R. Nisius[112], N. Nitika[69a,69c], J-E. Nitschke[50], E.K. Nkadimeng[34b], T. Nobe[159], T. Nommensen[153], M.B. Norfolk[145], B.J. Norman[35], M. Noury[36a], J. Novak[95], T. Novak[95], R. Novotny[135], L. Nozka[125], K. Ntekas[165], N.M.J. Nunes De Moura Junior[83b], J. Ocariz[130], A. Ochi[86], I. Ochoa[133a], S. Oerdek[48,z], J.T. Offermann[40], A. Ogrodnik[136], A. Oh[103], C.C. Ohm[150], H. Oide[84], M.L. Ojeda[37], Y. Okumura[159], L.F. Oleiro Seabra[133a], I. Oleksiyuk[56], G. Oliveira Correa[13], D. Oliveira Damazio[30], J.L. Oliver[165], Ö.O. Öncel[54], A.P. O'Neill[20], A. Onofre[133a,133e,e], P.U.E. Onyisi[11], M.J. Oreglia[40], D. Orestano[77a,77b], R. Orlandini[77a,77b], R.S. Orr[161], L.M. Osojnak[131], Y. Osumi[113], G. Otero y Garzon[31], H. Otono[90], G.J. Ottino[18a], M. Ouchrif[36d], F. Ould-Saada[128], T. Ovsiannikova[142], M. Owen[59], R.E. Owen[137], V.E. Ozcan[22a], F. Ozturk[88], N. Ozturk[8], S. Ozturk[82], H.A. Pacey[129], K. Pachal[162a], A. Pacheco Pages[13], C. Padilla Aranda[13], G. Padovano[75a,75b], S. Pagan Griso[18a], G. Palacino[68], A. Palazzo[70a,70b], J. Pampel[25], J. Pan[178], T. Pan[64a], D.K. Panchal[11], C.E. Pandini[60], J.G. Panduro Vazquez[137], H.D. Pandya[1], H. Pang[138], P. Pani[48], G. Panizzo[69a,69c], L. Panwar[130], L. Paolozzi[56], S. Parajuli[168],

A. Paramonov[6], C. Paraskevopoulos[53], D. Paredes Hernandez[64b], A. Pareti[73a,73b], K.R. Park[42], T.H. Park[112], F. Parodi[57b,57a], J.A. Parsons[42], U. Parzefall[54], B. Pascual Dias[41], L. Pascual Dominguez[101], E. Pasqualucci[75a], S. Passaggio[57b], F. Pastore[97], P. Patel[88], U.M. Patel[51], J.R. Pater[103], T. Pauly[37], F. Pauwels[136], C.I. Pazos[164], M. Pedersen[128], R. Pedro[133a], S.V. Peleganchuk[38], O. Penc[37], E.A. Pender[52], S. Peng[15], G.D. Penn[178], K.E. Penski[111], M. Penzin[38], B.S. Peralva[83d], A.P. Pereira Peixoto[142], L. Pereira Sanchez[149], D.V. Perepelitsa[30,ak], G. Perera[105], E. Perez Codina[37], M. Perganti[10], H. Pernegger[37], S. Perrella[75a,75b], O. Perrin[41], K. Peters[48], R.F.Y. Peters[103], B.A. Petersen[37], T.C. Petersen[43], E. Petit[104], V. Petousis[135], A.R. Petri[71a,71b], C. Petridou[158,d], T. Petru[136], A. Petrukhin[147], M. Pettee[18a], A. Petukhov[82], K. Petukhova[37], R. Pezoa[140f], L. Pezzotti[24b,24a], G. Pezzullo[178], L. Pfaffenbichler[37], A.J. Pfleger[37], T.M. Pham[176], T. Pham[107], P.W. Phillips[137], G. Piacquadio[151], E. Pianori[18a], F. Piazza[126], R. Piegaia[31], D. Pietreanu[28b], A.D. Pilkington[103], M. Pinamonti[69a,69c], J.L. Pinfold[2], B.C. Pinheiro Pereira[133a], J. Pinol Bel[13], A.E. Pinto Pinoargote[130], L. Pintucci[69a,69c], K.M. Piper[152], A. Pirttikoski[56], D.A. Pizzi[35], L. Pizzimento[64b], A. Plebani[33], M.-A. Pleier[30], V. Pleskot[136], E. Plotnikova[39], G. Poddar[96], R. Poettgen[100], L. Poggioli[130], S. Polacek[136], G. Polesello[73a], A. Poley[148], A. Polini[24b], C.S. Pollard[173], Z.B. Pollock[122], E. Pompa Pacchi[123], N.I. Pond[98], D. Ponomarenko[68], L. Pontecorvo[37], S. Popa[28a], G.A. Popeneciu[28d], A. Poreba[37], D.M. Portillo Quintero[162a], S. Pospisil[135], M.A. Postill[145], P. Postolache[28c], K. Potamianos[173], P.A. Potepa[87a], I.N. Potrap[39], C.J. Potter[33], H. Potti[153], J. Poveda[169], M.E. Pozo Astigarraga[37], R. Pozzi[37], A. Prades Ibanez[76a,76b], J. Pretel[171], D. Price[103], M. Primavera[70a], L. Primomo[69a,69c], M.A. Principe Martin[101], R. Privara[125], T. Procter[87b], M.L. Proffitt[142], N. Proklova[131], K. Prokofiev[64c], G. Proto[112], J. Proudfoot[6], M. Przybycien[87a], W.W. Przygoda[87b], A. Psallidas[46], J.E. Puddefoot[145], D. Pudzha[53], D. Pyatiizbyantseva[116], J. Qian[108], R. Qian[109], D. Qichen[103], Y. Qin[13], T. Qiu[52], A. Quadt[55], M. Queitsch-Maitland[103], G. Quetant[56], R.P. Quinn[170], G. Rabanal Bolanos[61], D. Rafanoharana[112], F. Raffaeli[76a,76b], F. Ragusa[71a,71b], J.L. Rainbolt[40], J.A. Raine[56], S. Rajagopalan[30], E. Ramakoti[39], L. Rambelli[57b,57a], I.A. Ramirez-Berend[35], K. Ran[48,114c], D.S. Rankin[131], N.P. Rapheeha[34g], H. Rasheed[28b], D.F. Rassloff[63a], A. Rastogi[18a], S. Rave[102], S. Ravera[57b,57a], B. Ravina[37], I. Ravinovich[175], M. Raymond[37], A.L. Read[128], N.P. Readioff[145], D.M. Rebuzzi[73a,73b], A.S. Reed[112], K. Reeves[27], J.A. Reidelsturz[177], D. Reikher[126], A. Rej[49], C. Rembser[37], H. Ren[62], M. Renda[28b], F. Renner[48], A.G. Rennie[59], A.L. Rescia[48], S. Resconi[71a], M. Ressegotti[57b,57a], S. Rettie[37], W.F. Rettie[35], E. Reynolds[18a], O.L. Rezanova[39], P. Reznicek[136], H. Riani[36d], N. Ribaric[51], E. Ricci[78a,78b], R. Richter[112], S. Richter[47a,47b], E. Richter-Was[87b], M. Ridel[130], S. Ridouani[36d], P. Rieck[120], P. Riedler[37], E.M. Riefel[47a,47b], J.O. Rieger[117], M. Rijssenbeek[151], M. Rimoldi[37], L. Rinaldi[24b,24a], P. Rincke[167,55], G. Ripellino[167], I. Riu[13], J.C. Rivera Vergara[171], F. Rizatdinova[124], E. Rizvi[96], B.R. Roberts[18a], S.S. Roberts[139], D. Robinson[33], M. Robles Manzano[102], A. Robson[59], A. Rocchi[76a,76b], C. Roda[74a,74b], S. Rodriguez Bosca[37], Y. Rodriguez Garcia[23a], A.M. Rodríguez Vera[118], S. Roe[37], J.T. Roemer[37], O. Røhne[128], R.A. Rojas[37], C.P.A. Roland[130], A. Romaniouk[79], E. Romano[73a,73b], M. Romano[24b], A.C. Romero Hernandez[168], N. Rompotis[94], L. Roos[130], S. Rosati[75a], B.J. Rosser[40], E. Rossi[129], E. Rossi[72a,72b], L.P. Rossi[61], L. Rossini[54], R. Rosten[122], M. Rotaru[28b], B. Rottler[54], D. Rousseau[66], D. Rousso[48], S. Roy-Garand[161], A. Rozanov[104], Z.M.A. Rozario[59], Y. Rozen[156], A. Rubio Jimenez[169], V.H. Ruelas Rivera[19], T.A. Ruggeri[1], A. Ruggiero[129], A. Ruiz-Martinez[169], A. Rummler[37], Z. Rurikova[54], N.A. Rusakovich[39], H.L. Russell[171], G. Russo[75a,75b], J.P. Rutherfoord[7], S. Rutherford Colmenares[33], M. Rybar[136], P. Rybczynski[87a], A. Ryzhov[45], J.A. Sabater Iglesias[56], H.F-W. Sadrozinski[139], F. Safai Tehrani[75a], S. Saha[1], M. Sahinsoy[82], B. Sahoo[175], A. Saibel[169], B.T. Saifuddin[123], M. Saimpert[138], G.T. Saito[83c], M. Saito[159], T. Saito[159], A. Sala[71a,71b], A. Salnikov[149], J. Salt[169], A. Salvador Salas[157], F. Salvatore[152], A. Salzburger[37], D. Sammel[54], E. Sampson[93], D. Sampsonidis[158,d], D. Sampsonidou[126], J. Sánchez[169], V. Sanchez Sebastian[169], H. Sandaker[128], C.O. Sander[48], J.A. Sandesara[176], M. Sandhoff[177], C. Sandoval[23b], L. Sanfilippo[63a], D.P.C. Sankey[137], T. Sano[89], A. Sansoni[53], L. Santi[37], C. Santoni[41], H. Santos[133a,133b], A. Santra[175], E. Sanzani[24b,24a], K.A. Saoucha[85b], J.G. Saraiva[133a,133d], J. Sardain[7], O. Sasaki[84], K. Sato[163], C. Sauer[37], E. Sauvan[4], P. Savard[161,ai], R. Sawada[159], C. Sawyer[137], L. Sawyer[99], C. Sbarra[24b], A. Sbrizzi[24b,24a], T. Scanlon[98], J. Schaarschmidt[142], U. Schäfer[102], A.C. Schaffer[66,45], D. Schaile[111], R.D. Schamberger[151], C. Scharf[19], M.M. Schefer[20], V.A. Schegelsky[38], D. Scheirich[136], M. Schernau[140e], C. Scheulen[56], C. Schiavi[57b,57a], M. Schioppa[44b,44a], B. Schlag[149], S. Schlenker[37], J. Schmeing[177], E. Schmidt[112], M.A. Schmidt[177], K. Schmieden[102], C. Schmitt[102], N. Schmitt[102], S. Schmitt[48], N.A. Schneider[111], L. Schoeffel[138], A. Schoening[63b], P.G. Scholer[35], E. Schopf[147], M. Schott[25], S. Schramm[56], T. Schroer[56], H-C. Schultz-Coulon[63a], M. Schumacher[54], B.A. Schumm[139], Ph. Schune[138], H.R. Schwartz[139], A. Schwartzman[149], T.A. Schwarz[108], Ph. Schwemling[138], R. Schwienhorst[109], F.G. Sciacca[20], A. Sciandra[30], G. Sciolla[27], F. Scuri[74a], C.D. Sebastiani[37], K. Sedlaczek[118], S.C. Seidel[115], A. Seiden[139], B.D. Seidlitz[42], C. Seitz[48], J.M. Seixas[83b], G. Sekhniaidze[72a], L. Selem[60], N. Semprini-Cesari[24b,24a], A. Semushin[179], D. Sengupta[56], V. Senthilkumar[169], L. Serin[66], M. Sessa[72a,72b], H. Severini[123], F. Sforza[57b,57a], A. Sfyrla[56], Q. Sha[14], E. Shabalina[55], H. Shaddix[118], A.H. Shah[33], R. Shaheen[150], J.D. Shahinian[131], M. Shamim[37], L.Y. Shan[14], M. Shapiro[18a], A. Sharma[37], A.S. Sharma[170], P. Sharma[30], P.B. Shatalov[38], K. Shaw[152], S.M. Shaw[103], Q. Shen[144a], D.J. Sheppard[148], P. Sherwood[98], L. Shi[98], X. Shi[14], S. Shimizu[84], C.O. Shimmin[178], I.P.J. Shipsey[129,*], S. Shirabe[90], M. Shiyakova[39,aa], M.J. Shochet[40], D.R. Shope[128], B. Shrestha[123], S. Shrestha[122,am], I. Shreyber[39], M.J. Shroff[171], P. Sicho[134], A.M. Sickles[168], E. Sideras Haddad[34g,166], A.C. Sidley[117], A. Sidoti[24b], F. Siegert[50], Dj. Sijacki[16], F. Sili[92], J.M. Silva[52], I. Silva Ferreira[83b], M.V. Silva Oliveira[30], S.B. Silverstein[47a], S. Simion[66], R. Simoniello[37], E.L. Simpson[103], H. Simpson[152], L.R. Simpson[6], S. Simsek[82], S. Sindhu[55], P. Sinervo[161], S.N. Singh[27], S. Singh[30], S. Sinha[48], S. Sinha[103], M. Sioli[24b,24a], K. Sioulas[9], I. Siral[37], E. Sitnikova[48], J. Sjölin[47a,47b], A. Skaf[55], E. Skorda[21], P. Skubic[123], M. Slawinska[88], I. Slazyk[17], I. Sliusar[128], V. Smakhtin[175], B.H. Smart[137], S.Yu. Smirnov[140b], Y. Smirnov[82], L.N. Smirnova[38,a], O. Smirnova[100], A.C. Smith[42], D.R. Smith[165], J.L. Smith[103], M.B. Smith[35], R. Smith[149], H. Smitmanns[102], M. Smizanska[93], K. Smolek[135], P. Smolyanskiy[135], A.A. Snesarev[39], H.L. Snoek[117], S. Snyder[30], R. Sobie[171,ac], A. Soffer[157], C.A. Solans Sanchez[37], E.Yu. Soldatov[39], U. Soldevila[169], A.A. Solodkov[34g], S. Solomon[27], A. Soloshenko[39], K. Solovieva[54], O.V. Solovyanov[41], P. Sommer[50], A. Sonay[13], A. Sopczak[135], A.L. Sopio[52], F. Sopkova[29b], J.D. Sorenson[115], I.R. Sotarriva Alvarez[141], V. Sothilingam[63a], O.J. Soto Sandoval[140c,140b], S. Sottocornola[68], R. Soualah[85a], Z. Soumaimi[36e], D. South[48], N. Soybelman[175], S. Spagnolo[70a,70b], M. Spalla[112], D. Sperlich[54], B. Spisso[72a,72b], D.P. Spiteri[59], L. Splendori[104], M. Spousta[136], E.J. Staats[35], R. Stamen[63a], E. Stanecka[88], W. Stanek-Maslouska[48], M.V. Stange[50], B. Stanislaus[18a], M.M. Stanitzki[48], B. Stapf[48], E.A. Starchenko[38], G.H. Stark[139], J. Stark[91], P. Staroba[134], P. Starovoitov[85b], R. Staszewski[88], G. Stavropoulos[46], A. Stefl[37], P. Steinberg[30], B. Stelzer[148,162a],

H.J. Stelzer[132], O. Stelzer[162a], H. Stenzel[58], T.J. Stevenson[152], G.A. Stewart[37], J.R. Stewart[124], M.C. Stockton[37], G. Stoicea[28b], M. Stolarski[133a], S. Stonjek[112], A. Straessner[50], J. Strandberg[150], S. Strandberg[47a,47b], M. Stratmann[177], M. Strauss[123], T. Strebler[104], P. Strizenec[29b], R. Ströhmer[172], D.M. Strom[126], R. Stroynowski[45], A. Strubig[47a,47b], S.A. Stucci[30], B. Stugu[17], J. Stupak[123], N.A. Styles[48], D. Su[149], S. Su[62], X. Su[62], D. Suchy[29a], K. Sugizaki[131], V.V. Sulin[38], M.J. Sullivan[94], D.M.S. Sultan[129], L. Sultanaliyeva[38], S. Sultansoy[3b], S. Sun[176], W. Sun[14], O. Sunneborn Gudnadottir[167], N. Sur[100], M.R. Sutton[152], H. Suzuki[163], M. Svatos[134], P.N. Swallow[33], M. Swiatlowski[162a], T. Swirski[172], A. Swoboda[37], I. Sykora[29a], M. Sykora[136], T. Sykora[136], D. Ta[102], K. Tackmann[48,z], A. Taffard[165], R. Tafirout[162a], Y. Takubo[84], M. Talby[104], A.A. Talyshev[38], K.C. Tam[64b], N.M. Tamir[157], A. Tanaka[159], J. Tanaka[159], R. Tanaka[66], M. Tanasini[151], Z. Tao[170], S. Tapia Araya[140f], S. Tapprogge[102], A. Tarek Abouelfadl Mohamed[109], S. Tarem[156], K. Tariq[14], G. Tarna[28b], G.F. Tartarelli[71a], M.J. Tartarin[91], P. Tas[136], M. Tasevsky[134], E. Tassi[44b,44a], A.C. Tate[168], G. Tateno[159], Y. Tayalati[36e,ab], G.N. Taylor[107], W. Taylor[162b], A.S. Tegetmeier[91], P. Teixeira-Dias[97], J.J. Teoh[161], K. Terashi[159], J. Terron[101], S. Terzo[13], M. Testa[53], R.J. Teuscher[161,ac], A. Thaler[79], O. Theiner[56], T. Theveneaux-Pelzer[104], D.W. Thomas[97], J.P. Thomas[21], E.A. Thompson[18a], P.D. Thompson[21], E. Thomson[131], R.E. Thornberry[45], C. Tian[62], Y. Tian[56], V. Tikhomirov[82], Yu.A. Tikhonov[39], S. Timoshenko[38], D. Timoshyn[136], E.X.L. Ting[1], P. Tipton[178], A. Tishelman-Charny[30], K. Todome[141], S. Todorova-Nova[136], S. Todt[50], L. Toffolin[69a,69c], M. Togawa[84], J. Tojo[90], S. Tokár[29a], O. Toldaiev[68], G. Tolkachev[104], M. Tomoto[84,113], L. Tompkins[149,o], E. Torrence[126], H. Torres[91], E. Torró Pastor[169], M. Toscani[31], C. Tosciri[40], M. Tost[11], D.R. Tovey[145], T. Trefzger[172], P.M. Tricarico[13], A. Tricoli[30], I.M. Trigger[162a], S. Trincaz-Duvoid[130], D.A. Trischuk[27], A. Tropina[39], L. Truong[34c], M. Trzebinski[88], A. Trzupek[88], F. Tsai[151], M. Tsai[108], A. Tsiamis[158], P.V. Tsiareshka[39], S. Tsigaridas[162a], A. Tsirigotis[158,v], V. Tsiskaridze[161], E.G. Tskhadadze[155a], M. Tsopoulou[158], Y. Tsujikawa[89], I.I. Tsukerman[38], V. Tsulaia[18a], S. Tsuno[84], K. Tsuri[121], D. Tsybychev[151], Y. Tu[64b], A. Tudorache[28b], V. Tudorache[28b], S.B. Tuncay[129], S. Turchikhin[57b,57a], I. Turk Cakir[3a], R. Turra[71a], T. Turtuvshin[39,ad], P.M. Tuts[42], S. Tzamarias[158,d], E. Tzovara[102], Y. Uematsu[84], F. Ukegawa[163], P.A. Ulloa Poblete[140c,140b], E.N. Umaka[30], G. Unal[37], A. Undrus[30], G. Unel[165], J. Urban[29b], P. Urrejola[140a], G. Usai[8], R. Ushioda[160], M. Usman[110], F. Ustuner[52], Z. Uysal[82], V. Vacek[135], B. Vachon[106], T. Vafeiadis[37], A. Vaitkus[98], C. Valderanis[111], E. Valdes Santurio[47a,47b], M. Valente[37], S. Valentinetti[24b,24a], A. Valero[169], E. Valiente Moreno[169], A. Vallier[91], J.A. Valls Ferrer[169], D.R. Van Arneman[117], T.R. Van Daalen[142], A. Van Der Graaf[49], H.Z. Van Der Schyf[34g], P. Van Gemmeren[6], M. Van Rijnbach[37], S. Van Stroud[98], I. Van Vulpen[117], P. Vana[136], M. Vanadia[76a,76b], U.M. Vande Voorde[150], W. Vandelli[37], E.R. Vandewall[124], D. Vannicola[157], L. Vannoli[53], R. Vari[75a], M. Varma[178], E.W. Varnes[7], C. Varni[18b], D. Varouchas[66], L. Varriale[169], K.E. Varvell[153], M.E. Vasile[28b], L. Vaslin[84], M.D. Vassilev[149], A. Vasyukov[39], L.M. Vaughan[124], R. Vavricka[136], T. Vazquez Schroeder[13], J. Veatch[32], V. Vecchio[103], M.J. Veen[105], I. Veliscek[30], I. Velkovska[95], L.M. Veloce[161], F. Veloso[133a,133c], S. Veneziano[75a], A. Ventura[70a,70b], S. Ventura Gonzalez[138], A. Verbytskyi[112], M. Verducci[74a,74b], C. Vergis[96], M. Verissimo De Araujo[83b], W. Verkerke[117], J.C. Vermeulen[117], C. Vernieri[149], M. Vessella[165], M.C. Vetterli[148,ai], A. Vgenopoulos[102], N. Viaux Maira[140f], T. Vickey[145], O.E. Vickey Boeriu[145], G.H.A. Viehhauser[129], L. Vigani[63b], M. Vigl[112], M. Villa[24b,24a], M. Villaplana Perez[169], E.M. Villhauer[40], E. Vilucchi[53], M. Vincent[169], M.G. Vincter[35], A. Visibile[117], C. Vittori[37], I. Vivarelli[24b,24a], E. Voevodina[112], F. Vogel[111], J.C. Voigt[50], P. Vokac[135], Yu. Volkotrub[87b], E. Von Toerne[25], B. Vormwald[37], K. Vorobev[51], M. Vos[169], K. Voss[147], M. Vozak[37], L. Vozdecky[123], N. Vranjes[16], M. Vranjes Milosavljevic[16], M. Vreeswijk[117], N.K. Vu[144b,144a], R. Vuillermet[37], O. Vujinovic[102], I. Vukotic[40], I.K. Vyas[35], J.F. Wack[33], S. Wada[163], C. Wagner[149], J.M. Wagner[18a], W. Wagner[177], S. Wahdan[177], H. Wahlberg[92], C.H. Waits[123], J. Walder[137], R. Walker[111], K. Walkingshaw Pass[59], W. Walkowiak[147], A. Wall[131], E.J. Wallin[100], T. Wamorkar[18a], A. Wang[62], A.Z. Wang[139], C. Wang[102], C. Wang[11], H. Wang[18a], J. Wang[64c], P. Wang[103], P. Wang[98], R. Wang[61], R. Wang[6], S.M. Wang[154], S. Wang[14], T. Wang[62], T. Wang[62], W.T. Wang[80], W. Wang[14], X. Wang[168], X. Wang[144a], X. Wang[48], Y. Wang[114a], Y. Wang[62], Z. Wang[108], Z. Wang[144b], Z. Wang[108], C. Wanotayaroj[84], A. Warburton[106], A.L. Warnerbring[147], N. Warrack[59], S. Waterhouse[97], A.T. Watson[21], H. Watson[52], M.F. Watson[21], E. Watton[59], G. Watts[142], B.M. Waugh[98], J.M. Webb[54], C. Weber[30], H.A. Weber[19], M.S. Weber[20], S.M. Weber[63a], C. Wei[62], Y. Wei[54], A.R. Weidberg[129], E.J. Weik[120], J. Weingarten[49], C. Weiser[54], C.J. Wells[48], T. Wenaus[30], B. Wendland[49], T. Wengler[37], N.S. Wenke[112], N. Wermes[25], M. Wessels[63a], A.M. Wharton[93], A.S. White[61], A. White[8], M.J. White[1], D. Whiteson[165], L. Wickremasinghe[127], W. Wiedenmann[176], M. Wielers[137], R. Wierda[150], C. Wiglesworth[43], H.G. Wilkens[37], J.J.H. Wilkinson[33], D.M. Williams[42], H.H. Williams[131], S. Williams[33], S. Willocq[105], B.J. Wilson[103], D.J. Wilson[103], P.J. Windischhofer[40], F.I. Winkel[31], F. Winklmeier[126], B.T. Winter[54], M. Wittgen[149], M. Wobisch[99], T. Wojtkowski[60], Z. Wolffs[117], J. Wollrath[37], M.W. Wolter[88], H. Wolters[133a,133c], M.C. Wong[139], E.L. Woodward[42], S.D. Worm[48], B.K. Wosiek[88], K.W. Woźniak[88], S. Wozniewski[55], K. Wraight[59], C. Wu[161], C. Wu[21], J. Wu[159], M. Wu[114b], M. Wu[116], S.L. Wu[176], S. Wu[14], X. Wu[62], Y. Wu[62], Z. Wu[4], J. Wuerzinger[112], T.R. Wyatt[103], B.M. Wynne[52], S. Xella[43], L. Xia[114a], M. Xia[15], M. Xie[62], A. Xiong[126], J. Xiong[18a], D. Xu[14], H. Xu[62], L. Xu[62], R. Xu[131], T. Xu[108], Y. Xu[142], Z. Xu[52], Z. Xu[114a], B. Yabsley[153], S. Yacoob[34a], Y. Yamaguchi[84], E. Yamashita[159], H. Yamauchi[163], T. Yamazaki[18a], Y. Yamazaki[86], S. Yan[59], Z. Yan[105], C. Yang[18a], H.J. Yang[144a,144b], H.T. Yang[62], S. Yang[62], T. Yang[64c], X. Yang[37], X. Yang[14], Y. Yang[159], Y. Yang[62], W-M. Yao[18a], C.L. Yardley[152], J. Ye[14], S. Ye[30], X. Ye[62], Y. Yeh[98], I. Yeletskikh[39], B. Yeo[18b], M.R. Yexley[98], T.P. Yildirim[129], P. Yin[42], K. Yorita[174], C.J.S. Young[37], C. Young[149], N.D. Young[126], Y. Yu[62], J. Yuan[14,114c], M. Yuan[108], R. Yuan[144b,144a], L. Yue[98], M. Zaazoua[62], B. Zabinski[88], I. Zahir[36a], A. Zaio[57b,57a], Z.K. Zak[88], T. Zakareishvili[169], S. Zambito[56], J.A. Zamora Saa[140d], J. Zang[159], R. Zanzottera[71a,71b], O. Zaplatilek[135], C. Zeitnitz[177], H. Zeng[14], J.C. Zeng[168], D.T. Zenger Jr[27], O. Zenin[38], T. Ženiš[29a], S. Zenz[96], D. Zerwas[66], M. Zhai[14,114c], D.F. Zhang[145], G. Zhang[14], J. Zhang[143a], J. Zhang[6], K. Zhang[14,114c], L. Zhang[62], L. Zhang[114a], P. Zhang[14,114c], R. Zhang[114a], S. Zhang[91], T. Zhang[159], Y. Zhang[142], Y. Zhang[98], Y. Zhang[62], Y. Zhang[114a], Z. Zhang[143a], Z. Zhang[66], H. Zhao[142], T. Zhao[143a], Y. Zhao[35], Z. Zhao[62], Z. Zhao[62], A. Zhemchugov[39], J. Zheng[114a], K. Zheng[168], X. Zheng[62], Z. Zheng[149], D. Zhong[168], B. Zhou[108], H. Zhou[7], N. Zhou[144a], Y. Zhou[15], Y. Zhou[114a], Y. Zhou[7], C.G. Zhu[143a], J. Zhu[108], X. Zhu[144b], Y. Zhu[144a], Y. Zhu[62], X. Zhuang[14], K. Zhukov[68], N.I. Zimine[39], J. Zinsser[63b], M. Ziolkowski[147], L. Živković[16], A. Zoccoli[24b,24a], K. Zoch[61], A. Zografos[37], T.G. Zorbas[145], O. Zormpa[46], L. Zwalinski[37]

[1]Department of Physics, University of Adelaide, Adelaide, Australia.
[2]Department of Physics, University of Alberta, Edmonton AB, Canada.
[3](a)Department of Physics, Ankara University, Ankara; (b)Division of Physics, TOBB University of Economics and Technology, Ankara, Türkiye.
[4]LAPP, Université Savoie Mont Blanc, CNRS/IN2P3, Annecy, France.
[5]APC, Université Paris Cité, CNRS/IN2P3, Paris, France.
[6]High Energy Physics Division, Argonne National Laboratory, Argonne IL, United States of America.
[7]Department of Physics, University of Arizona, Tucson AZ, United States of America.
[8]Department of Physics, University of Texas at Arlington, Arlington TX, United States of America.
[9]Physics Department, National and Kapodistrian University of Athens, Athens, Greece.
[10]Physics Department, National Technical University of Athens, Zografou, Greece.
[11]Department of Physics, University of Texas at Austin, Austin TX, United States of America.
[12]Institute of Physics, Azerbaijan Academy of Sciences, Baku, Azerbaijan.
[13]Institut de Física d'Altes Energies (IFAE), Barcelona Institute of Science and Technology, Barcelona; Spain.
[14]Institute of High Energy Physics, Chinese Academy of Sciences, Beijing, China.
[15]Physics Department, Tsinghua University, Beijing, China.
[16]Institute of Physics, University of Belgrade, Belgrade, Serbia.
[17]Department for Physics and Technology, University of Bergen, Bergen, Norway.
[18](a)Physics Division, Lawrence Berkeley National Laboratory, Berkeley CA; (b)University of California, Berkeley CA, United States of America.
[19]Institut für Physik, Humboldt Universität zu Berlin, Berlin, Germany.
[20]Albert Einstein Center for Fundamental Physics and Laboratory for High Energy Physics, University of Bern, Bern, Switzerland.
[21]School of Physics and Astronomy, University of Birmingham, Birmingham, United Kingdom.
[22](a)Department of Physics, Bogazici University, Istanbul; (b)Department of Physics Engineering, Gaziantep University, Gaziantep; (c)Department of Physics, Istanbul University, Istanbul, Türkiye.
[23](a)Facultad de Ciencias y Centro de Investigaciónes, Universidad Antonio Nariño, Bogotá; (b)Departamento de Física, Universidad Nacional de Colombia, Bogotá, Colombia.
[24](a)Dipartimento di Fisica e Astronomia A. Righi, Università di Bologna, Bologna, Italy; (b)INFN Sezione di Bologna, Italy.
[25]Physikalisches Institut, Universität Bonn, Bonn, Germany.
[26]Department of Physics, Boston University, Boston MA, United States of America.
[27]Department of Physics, Brandeis University, Waltham MA, United States of America.
[28](a)Transilvania University of Brasov, Brasov; (b)Horia Hulubei National Institute of Physics and Nuclear Engineering, Bucharest; (c)Department of Physics, Alexandru Ioan Cuza University of Iasi, Iasi; (d)National Institute for Research and Development of Isotopic and Molecular Technologies, Physics Department, Cluj-Napoca; (e)National University of Science and Technology Politechnica, Bucharest; (f)West University in Timisoara, Timisoara; (g)Faculty of Physics, University of Bucharest, Bucharest, Romania.
[29](a)Faculty of Mathematics, Physics and Informatics, Comenius University, Bratislava; (b)Department of Subnuclear Physics, Institute of Experimental Physics of the Slovak Academy of Sciences, Kosice, Slovak Republic.
[30]Physics Department, Brookhaven National Laboratory, Upton NY, United States of America.
[31]Universidad de Buenos Aires, Facultad de Ciencias Exactas y Naturales, Departamento de Física, y CONICET, Instituto de Física de Buenos Aires (IFIBA), Buenos Aires, Argentina.
[32]California State University, CA, United States of America.
[33]Cavendish Laboratory, University of Cambridge, Cambridge, United Kingdom.
[34](a)Department of Physics, University of Cape Town, Cape Town; (b)iThemba Labs, Western Cape; (c)Department of Mechanical Engineering Science, University of Johannesburg, Johannesburg; (d)National Institute of Physics, University of the Philippines Diliman (Philippines); (e)University of South Africa, Department of Physics, Pretoria; (f)University of Zululand, KwaDlangezwa; (g)School of Physics, University of the Witwatersrand, Johannesburg, South Africa.
[35]Department of Physics, Carleton University, Ottawa ON, Canada.
[36](a)Faculté des Sciences Ain Chock, Université Hassan II de Casablanca; (b)Faculté des Sciences, Université Ibn-Tofail, Kénitra; (c)Faculté des Sciences Semlalia, Université Cadi Ayyad, LPHEA-Marrakech; (d)LPMR, Faculté des Sciences, Université Mohamed Premier, Oujda; (e)Faculté des sciences, Université Mohammed V, Rabat; (f)Institute of Applied Physics, Mohammed VI Polytechnic University, Ben Guerir, Morocco.
[37]CERN, Geneva, Switzerland.
[38]Affiliated with an institute formerly covered by a cooperation agreement with CERN.
[39]Affiliated with an international laboratory covered by a cooperation agreement with CERN.
[40]Enrico Fermi Institute, University of Chicago, Chicago IL, United States of America.
[41]LPC, Université Clermont Auvergne, CNRS/IN2P3, Clermont-Ferrand, France.
[42]Nevis Laboratory, Columbia University, Irvington NY, United States of America.
[43]Niels Bohr Institute, University of Copenhagen, Copenhagen, Denmark.
[44](a)Dipartimento di Fisica, Università della Calabria, Rende; (b)INFN Gruppo Collegato di Cosenza, Laboratori Nazionali di Frascati, Italy.
[45]Physics Department, Southern Methodist University, Dallas TX, United States of America.
[46]National Centre for Scientific Research "Demokritos", Agia Paraskevi, Greece.
[47](a)Department of Physics, Stockholm University; (b)Oskar Klein Centre, Stockholm, Sweden.
[48]Deutsches Elektronen-Synchrotron DESY, Hamburg and Zeuthen, Germany.
[49]Fakultät Physik , Technische Universität Dortmund, Dortmund, Germany.
[50]Institut für Kern- und Teilchenphysik, Technische Universität Dresden, Dresden, Germany.
[51]Department of Physics, Duke University, Durham NC, United States of America.
[52]SUPA - School of Physics and Astronomy, University of Edinburgh, Edinburgh, United Kingdom.
[53]INFN e Laboratori Nazionali di Frascati, Frascati, Italy.
[54]Physikalisches Institut, Albert-Ludwigs-Universität Freiburg, Freiburg, Germany.
[55]II. Physikalisches Institut, Georg-August-Universität Göttingen, Göttingen, Germany.
[56]Département de Physique Nucléaire et Corpusculaire, Université de Genève, Genève, Switzerland.
[57](a)Dipartimento di Fisica, Università di Genova, Genova; (b)INFN Sezione di Genova, Italy.
[58]II. Physikalisches Institut, Justus-Liebig-Universität Giessen, Giessen, Germany.
[59]SUPA - School of Physics and Astronomy, University of Glasgow, Glasgow, United Kingdom.
[60]LPSC, Université Grenoble Alpes, CNRS/IN2P3, Grenoble INP, Grenoble, France.
[61]Laboratory for Particle Physics and Cosmology, Harvard University, Cambridge MA, United States of America.

[62]Department of Modern Physics and State Key Laboratory of Particle Detection and Electronics, University of Science and Technology of China, Hefei, China.
[63](a)Kirchhoff-Institut für Physik, Ruprecht-Karls-Universität Heidelberg, Heidelberg; (b)Physikalisches Institut, Ruprecht-Karls-Universität Heidelberg, Heidelberg, Germany.
[64](a)Department of Physics, Chinese University of Hong Kong, Shatin, N.T., Hong Kong; (b)Department of Physics, University of Hong Kong, Hong Kong; (c)Department of Physics and Institute for Advanced Study, Hong Kong University of Science and Technology, Clear Water Bay, Kowloon, Hong Kong, China.
[65]Department of Physics, National Tsing Hua University, Hsinchu, Taiwan.
[66]IJCLab, Université Paris-Saclay, CNRS/IN2P3, 91405, Orsay, France.
[67]Centro Nacional de Microelectrónica (IMB-CNM-CSIC), Barcelona, Spain.
[68]Department of Physics, Indiana University, Bloomington IN, United States of America.
[69](a)INFN Gruppo Collegato di Udine, Sezione di Trieste, Udine; (b)ICTP, Trieste; (c)Dipartimento Politecnico di Ingegneria e Architettura, Università di Udine, Udine, Italy.
[70](a)INFN Sezione di Lecce; (b)Dipartimento di Matematica e Fisica, Università del Salento, Lecce, Italy.
[71](a)INFN Sezione di Milano; (b)Dipartimento di Fisica, Università di Milano, Milano, Italy.
[72](a)INFN Sezione di Napoli; (b)Dipartimento di Fisica, Università di Napoli, Napoli, Italy.
[73](a)INFN Sezione di Pavia; (b)Dipartimento di Fisica, Università di Pavia, Pavia, Italy.
[74](a)INFN Sezione di Pisa; (b)Dipartimento di Fisica E. Fermi, Università di Pisa, Pisa, Italy.
[75](a)INFN Sezione di Roma; (b)Dipartimento di Fisica, Sapienza Università di Roma, Roma, Italy.
[76](a)INFN Sezione di Roma Tor Vergata; (b)Dipartimento di Fisica, Università di Roma Tor Vergata, Roma, Italy.
[77](a)INFN Sezione di Roma Tre; (b)Dipartimento di Matematica e Fisica, Università Roma Tre, Roma, Italy.
[78](a)INFN-TIFPA; (b)Università degli Studi di Trento, Trento, Italy.
[79]Universität Innsbruck, Department of Astro and Particle Physics, Innsbruck, Austria.
[80]University of Iowa, Iowa City IA, United States of America.
[81]Department of Physics and Astronomy, Iowa State University, Ames IA, United States of America.
[82]Istinye University, Sariyer, Istanbul, Türkiye.
[83](a)Departamento de Engenharia Elétrica, Universidade Federal de Juiz de Fora (UFJF), Juiz de Fora; (b)Universidade Federal do Rio De Janeiro COPPE/EE/IF, Rio de Janeiro; (c)Instituto de Física, Universidade de São Paulo, São Paulo; (d)Rio de Janeiro State University, Rio de Janeiro; (e)Federal University of Bahia, Bahia, Brazil.
[84]KEK, High Energy Accelerator Research Organization, Tsukuba, Japan.
[85](a)Khalifa University of Science and Technology, Abu Dhabi; (b)University of Sharjah, Sharjah, United Arab Emirates.
[86]Graduate School of Science, Kobe University, Kobe, Japan.
[87](a)AGH University of Krakow, Faculty of Physics and Applied Computer Science, Krakow; (b)Marian Smoluchowski Institute of Physics, Jagiellonian University, Krakow, Poland.
[88]Institute of Nuclear Physics Polish Academy of Sciences, Krakow, Poland.
[89]Faculty of Science, Kyoto University, Kyoto, Japan.
[90]Research Center for Advanced Particle Physics and Department of Physics, Kyushu University, Fukuoka , Japan.
[91]L2IT, Université de Toulouse, CNRS/IN2P3, UPS, Toulouse, France.
[92]Instituto de Física La Plata, Universidad Nacional de La Plata and CONICET, La Plata, Argentina.
[93]Physics Department, Lancaster University, Lancaster, United Kingdom.
[94]Oliver Lodge Laboratory, University of Liverpool, Liverpool, United Kingdom.
[95]Department of Experimental Particle Physics, Jožef Stefan Institute and Department of Physics, University of Ljubljana, Ljubljana, Slovenia.
[96]Department of Physics and Astronomy, Queen Mary University of London, London, United Kingdom.
[97]Department of Physics, Royal Holloway University of London, Egham, United Kingdom.
[98]Department of Physics and Astronomy, University College London, London, United Kingdom.
[99]Louisiana Tech University, Ruston LA, United States of America.
[100]Fysiska institutionen, Lunds universitet, Lund, Sweden.
[101]Departamento de Física Teorica C-15 and CIAFF, Universidad Autónoma de Madrid, Madrid, Spain.
[102]Institut für Physik, Universität Mainz, Mainz, Germany.
[103]School of Physics and Astronomy, University of Manchester, Manchester, United Kingdom.
[104]CPPM, Aix-Marseille Université, CNRS/IN2P3, Marseille, France.
[105]Department of Physics, University of Massachusetts, Amherst MA, United States of America.
[106]Department of Physics, McGill University, Montreal QC, Canada.
[107]School of Physics, University of Melbourne, Victoria, Australia.
[108]Department of Physics, University of Michigan, Ann Arbor MI, United States of America.
[109]Department of Physics and Astronomy, Michigan State University, East Lansing MI, United States of America.
[110]Group of Particle Physics, University of Montreal, Montreal QC, Canada.
[111]Fakultät für Physik, Ludwig-Maximilians-Universität München, München, Germany.
[112]Max-Planck-Institut für Physik (Werner-Heisenberg-Institut), München, Germany.
[113]Graduate School of Science and Kobayashi-Maskawa Institute, Nagoya University, Nagoya, Japan.
[114](a)Department of Physics, Nanjing University, Nanjing; (b)School of Science, Shenzhen Campus of Sun Yat-sen University; (c)University of Chinese Academy of Science (UCAS), Beijing, China.
[115]Department of Physics and Astronomy, University of New Mexico, Albuquerque NM, United States of America.
[116]Institute for Mathematics, Astrophysics and Particle Physics, Radboud University/Nikhef, Nijmegen, Netherlands.
[117]Nikhef National Institute for Subatomic Physics and University of Amsterdam, Amsterdam, Netherlands.
[118]Department of Physics, Northern Illinois University, DeKalb IL, United States of America.
[119](a)New York University Abu Dhabi, Abu Dhabi; (b)United Arab Emirates University, Al Ain, United Arab Emirates.
[120]Department of Physics, New York University, New York NY, United States of America.
[121]Ochanomizu University, Otsuka, Bunkyo-ku, Tokyo, Japan.
[122]Ohio State University, Columbus OH, United States of America.
[123]Homer L. Dodge Department of Physics and Astronomy, University of Oklahoma, Norman OK, United States of America.
[124]Department of Physics, Oklahoma State University, Stillwater OK, United States of America.
[125]Palacký University, Joint Laboratory of Optics, Olomouc, Czech Republic.
[126]Institute for Fundamental Science, University of Oregon, Eugene, OR, United States of America.
[127]Graduate School of Science, University of Osaka, Osaka, Japan.
[128]Department of Physics, University of Oslo, Oslo, Norway.
[129]Department of Physics, Oxford University, Oxford, United Kingdom.

[130]LPNHE, Sorbonne Université, Université Paris Cité, CNRS/IN2P3, Paris, France.
[131]Department of Physics, University of Pennsylvania, Philadelphia PA, United States of America.
[132]Department of Physics and Astronomy, University of Pittsburgh, Pittsburgh PA, United States of America.
[133(a)]Laboratório de Instrumentação e Física Experimental de Partículas - LIP, Lisboa; [(b)]Departamento de Física, Faculdade de Ciências, Universidade de Lisboa, Lisboa; [(c)]Departamento de Física, Universidade de Coimbra, Coimbra; [(d)]Centro de Física Nuclear da Universidade de Lisboa, Lisboa; [(e)]Departamento de Física, Escola de Ciências, Universidade do Minho, Braga; [(f)]Departamento de Física Teórica y del Cosmos, Universidad de Granada, Granada (Spain); [(g)]Departamento de Física, Instituto Superior Técnico, Universidade de Lisboa, Lisboa, Portugal.
[134]Institute of Physics of the Czech Academy of Sciences, Prague, Czech Republic.
[135]Czech Technical University in Prague, Prague, Czech Republic.
[136]Charles University, Faculty of Mathematics and Physics, Prague, Czech Republic.
[137]Particle Physics Department, Rutherford Appleton Laboratory, Didcot, United Kingdom.
[138]IRFU, CEA, Université Paris-Saclay, Gif-sur-Yvette, France.
[139]Santa Cruz Institute for Particle Physics, University of California Santa Cruz, Santa Cruz CA, United States of America.
[140(a)]Departamento de Física, Pontificia Universidad Católica de Chile, Santiago; [(b)]Millennium Institute for Subatomic physics at high energy frontier (SAPHIR), Santiago; [(c)]Instituto de Investigación Multidisciplinario en Ciencia y Tecnología, y Departamento de Física, Universidad de La Serena; [(d)]Universidad Andres Bello, Department of Physics, Santiago; [(e)]Instituto de Alta Investigación, Universidad de Tarapacá, Arica; [(f)]Departamento de Física, Universidad Técnica Federico Santa María, Valparaíso, Chile.
[141]Department of Physics, Institute of Science, Tokyo, Japan.
[142]Department of Physics, University of Washington, Seattle WA, United States of America.
[143(a)]Institute of Frontier and Interdisciplinary Science and Key Laboratory of Particle Physics and Particle Irradiation (MOE), Shandong University, Qingdao; [(b)]School of Physics, Zhengzhou University, China.
[144(a)]State Key Laboratory of Dark Matter Physics, School of Physics and Astronomy, Shanghai Jiao Tong University, Key Laboratory for Particle Astrophysics and Cosmology (MOE), SKLPPC, Shanghai; [(b)]State Key Laboratory of Dark Matter Physics, Tsung-Dao Lee Institute, Shanghai Jiao Tong University, Shanghai, China.
[145]Department of Physics and Astronomy, University of Sheffield, Sheffield, United Kingdom.
[146]Department of Physics, Shinshu University, Nagano, Japan.
[147]Department Physik, Universität Siegen, Siegen, Germany.
[148]Department of Physics, Simon Fraser University, Burnaby BC, Canada.
[149]SLAC National Accelerator Laboratory, Stanford CA, United States of America.
[150]Department of Physics, Royal Institute of Technology, Stockholm, Sweden.
[151]Departments of Physics and Astronomy, Stony Brook University, Stony Brook NY, United States of America.
[152]Department of Physics and Astronomy, University of Sussex, Brighton, United Kingdom.
[153]School of Physics, University of Sydney, Sydney, Australia.
[154]Institute of Physics, Academia Sinica, Taipei, Taiwan.
[155(a)]E. Andronikashvili Institute of Physics, Iv. Javakhishvili Tbilisi State University, Tbilisi; [(b)]High Energy Physics Institute, Tbilisi State University, Tbilisi; [(c)]University of Georgia, Tbilisi, Georgia.
[156]Department of Physics, Technion, Israel Institute of Technology, Haifa, Israel.
[157]Raymond and Beverly Sackler School of Physics and Astronomy, Tel Aviv University, Tel Aviv, Israel.
[158]Department of Physics, Aristotle University of Thessaloniki, Thessaloniki, Greece.
[159]International Center for Elementary Particle Physics and Department of Physics, University of Tokyo, Tokyo, Japan.
[160]Graduate School of Science and Technology, Tokyo Metropolitan University, Tokyo, Japan.
[161]Department of Physics, University of Toronto, Toronto ON, Canada.
[162(a)]TRIUMF, Vancouver BC; [(b)]Department of Physics and Astronomy, York University, Toronto ON, Canada.
[163]Division of Physics and Tomonaga Center for the History of the Universe, Faculty of Pure and Applied Sciences, University of Tsukuba, Tsukuba, Japan.
[164]Department of Physics and Astronomy, Tufts University, Medford MA, United States of America.
[165]Department of Physics and Astronomy, University of California Irvine, Irvine CA, United States of America.
[166]University of West Attica, Athens, Greece.
[167]Department of Physics and Astronomy, University of Uppsala, Uppsala, Sweden.
[168]Department of Physics, University of Illinois, Urbana IL, United States of America.
[169]Instituto de Física Corpuscular (IFIC), Centro Mixto Universidad de Valencia - CSIC, Valencia, Spain.
[170]Department of Physics, University of British Columbia, Vancouver BC, Canada.
[171]Department of Physics and Astronomy, University of Victoria, Victoria BC, Canada.
[172]Fakultät für Physik und Astronomie, Julius-Maximilians-Universität Würzburg, Würzburg, Germany.
[173]Department of Physics, University of Warwick, Coventry, United Kingdom.
[174]Waseda University, Tokyo, Japan.
[175]Department of Particle Physics and Astrophysics, Weizmann Institute of Science, Rehovot, Israel.
[176]Department of Physics, University of Wisconsin, Madison WI, United States of America.
[177]Fakultät für Mathematik und Naturwissenschaften, Fachgruppe Physik, Bergische Universität Wuppertal, Wuppertal, Germany.
[178]Department of Physics, Yale University, New Haven CT, United States of America.
[179]Yerevan Physics Institute, Yerevan, Armenia.

[a] Also at Affiliated with an institute formerly covered by a cooperation agreement with CERN.
[b] Also at An-Najah National University, Nablus, Palestine.
[c] Also at Borough of Manhattan Community College, City University of New York, New York NY, United States of America.
[d] Also at Center for Interdisciplinary Research and Innovation (CIRI-AUTH), Thessaloniki, Greece.
[e] Also at Centre of Physics of the Universities of Minho and Porto (CF-UM-UP), Portugal.
[f] Also at CERN, Geneva, Switzerland.
[g] Also at CMD-AC UNEC Research Center, Azerbaijan State University of Economics (UNEC), Azerbaijan.
[h] Also at Département de Physique Nucléaire et Corpusculaire, Université de Genève, Genève, Switzerland.
[i] Also at Departament de Fisica de la Universitat Autonoma de Barcelona, Barcelona, Spain.
[j] Also at Department of Financial and Management Engineering, University of the Aegean, Chios, Greece.
[k] Also at Department of Mathematical Sciences, University of South Africa, Johannesburg, South Africa.
[l] Also at Department of Modern Physics and State Key Laboratory of Particle Detection and Electronics, University of Science and Technology of China, Hefei, China.

[m] Also at Department of Physics, Bolu Abant Izzet Baysal University, Bolu, Türkiye.
[n] Also at Department of Physics, King's College London, London, United Kingdom.
[o] Also at Department of Physics, Stanford University, Stanford CA, United States of America.
[p] Also at Department of Physics, Stellenbosch University, South Africa.
[q] Also at Department of Physics, University of Fribourg, Fribourg, Switzerland.
[r] Also at Department of Physics, University of Thessaly, Greece.
[s] Also at Department of Physics, Westmont College, Santa Barbara, United States of America.
[t] Also at Faculty of Physics, Sofia University, 'St. Kliment Ohridski', Sofia, Bulgaria.
[u] Also at Faculty of Physics, University of Bucharest , Romania.
[v] Also at Hellenic Open University, Patras, Greece.
[w] Also at Henan University, China.
[x] Also at Imam Mohammad Ibn Saud Islamic University, Saudi Arabia.
[y] Also at Institucio Catalana de Recerca i Estudis Avancats, ICREA, Barcelona, Spain.
[z] Also at Institut für Experimentalphysik, Universität Hamburg, Hamburg, Germany.
[aa] Also at Institute for Nuclear Research and Nuclear Energy (INRNE) of the Bulgarian Academy of Sciences, Sofia, Bulgaria.
[ab] Also at Institute of Applied Physics, Mohammed VI Polytechnic University, Ben Guerir, Morocco.
[ac] Also at Institute of Particle Physics (IPP), Canada.
[ad] Also at Institute of Physics and Technology, Mongolian Academy of Sciences, Ulaanbaatar, Mongolia.
[ae] Also at Institute of Physics, Azerbaijan Academy of Sciences, Baku, Azerbaijan.
[af] Also at Institute of Theoretical Physics, Ilia State University, Tbilisi, Georgia.
[ag] Also at National Institute of Physics, University of the Philippines Diliman (Philippines), Philippines.
[ah] Also at The Collaborative Innovation Center of Quantum Matter (CICQM), Beijing, China.
[ai] Also at TRIUMF, Vancouver BC, Canada.
[aj] Also at Università di Napoli Parthenope, Napoli, Italy.
[ak] Also at University of Colorado Boulder, Department of Physics, Colorado, United States of America.
[al] Also at University of Sienna, Italy.
[am] Also at Washington College, Chestertown, MD, United States of America.
[an] Also at Yeditepe University, Physics Department, Istanbul, Türkiye.

[†]Deceased

References

[1] ATLAS Collaboration, Observation of a new particle in the search for the Standard Model Higgs boson with the ATLAS detector at the LHC, Phys. Lett. B 716 (2012) 1. 1207.7214. https://doi.org/10.1016/j.physletb.2012.08.020
[2] CMS Collaboration, Observation of a new boson at a mass of 125 GeV with the CMS experiment at the LHC, Phys. Lett. B 716 (2012) 30. 1207.7235. https://doi.org/10.1016/j.physletb.2012.08.021
[3] K. Agashe, R. Contino, A. Pomarol, The minimal composite Higgs model, Nucl. Phys. B 719 (1-2) (2005) 165–187.
[4] G.C. Branco, P.M. Ferreira, L. Lavoura, M.N. Rebelo, M. Sher, J.P. Silva, Theory and phenomenology of two-Higgs-doublet models, Phys. Rep. 516 (1-2) (2012) 1–102.
[5] Q.H. Cao, H.L. Li, L.X. Xu, J.H. Yu, What can we learn from the total width of the Higgs boson?, Chin. Phys. C 47 (3) (2023) 033101. 2107.08343. https://doi.org/10.1088/1674-1137/aca8f6
[6] D. de Florian, et al., LHC Higgs Cross Section Working Group, Handbook of LHC Higgs Cross Sections: 4. Deciphering the Nature of the Higgs Sector (2017). 1610.07922. https://doi.org/10.23731/CYRM-2017-002
[7] CMS Collaboration, Measurement of the Higgs boson mass and width using the four-lepton final state in proton–proton collisions at $\sqrt{s} = 13$ TeV, Phys. Rev. D 111 (2024) 092014. 2409.13663. https://doi.org/10.1103/PhysRevD.111.092014
[8] ATLAS Collaboration, Measurement of the Higgs boson mass in the $H \to ZZ^* \to 4\ell$ decay channel using 139 fb^{-1} of $\sqrt{s} = 13$ TeV pp collisions recorded by the ATLAS detector at the LHC, Phys. Lett. B 843 (2023) 137880. 2207.00320. https://doi.org/10.1016/j.physletb.2023.137880
[9] G. Passarino, Higgs interference effects in $gg \to ZZ$ and their uncertainty, JHEP 08 (2012) 146. 1206.3824. https://doi.org/10.1007/JHEP08(2012)146
[10] J.M. Campbell, R.K. Ellis, C. Williams, Bounding the Higgs width at the LHC: Complementary results from $H \to WW$, Phys. Rev. D 89 (2014) 053011. 1312.1628. https://doi.org/10.1103/PhysRevD.89.053011
[11] F. Caola, K. Melnikov, Constraining the Higgs boson width with ZZ production at the LHC, Phys. Rev. D 88 (2013) 054024. 1307.4935. https://doi.org/10.1103/PhysRevD.88.054024
[12] H. Georgi, M. Machacek, Doubly charged Higgs bosons, Nucl. Phys. B 262 (3) (1985) 463–477.
[13] R. Alonso, E.E. Jenkins, A.V. Manohar, Sigma models with negative curvature, Phys. Lett. B 756 (2016) 358–364.
[14] ATLAS Collaboration, Measurement of off-shell Higgs boson production in the $H^* \to ZZ \to 4\ell$ decay channel using a neural simulation-based inference technique in 13 TeV pp collisions with the ATLAS detector, Rept. Prog. Phys. 88 (2025) 057803. 2412.01548. https://doi.org/10.1088/1361-6633/adcd9a
[15] CMS Collaboration, Measurement of the Higgs boson width and evidence of its off-shell contributions to ZZ production, Nat. Phys. 18 (2022) 1329–1334. 2202.06923. https://doi.org/10.1038/s41567-022-01682-0
[16] ATLAS Collaboration, Constraint on the total width of the Higgs boson from Higgs boson and four-top-quark measurements in pp collisions at $\sqrt{s} = 13$ TeV with the ATLAS detector, Phys. Lett. B 861 (2025) 139277. 2407.10631. https://doi.org/10.1016/j.physletb.2025.139277
[17] ATLAS Collaboration, Constraints on the off-shell Higgs boson signal strength in the high-mass ZZ and WW final states with the ATLAS detector, Eur. Phys. J. C 75 (2015) 335. 1503.01060. https://doi.org/10.1140/epjc/s10052-015-3542-2
[18] CMS Collaboration, Search for Higgs boson off-shell production in proton –proton collisions at 7 and 8 TeV and derivation of constraints on its total decay width, JHEP 09 (2016) 051. 1605.02329. https://doi.org/10.1007/JHEP09(2016)051
[19] M.A. Solberg, On the terms violating the custodial symmetry in multi-Higgs-doublet models, J. Phys. G 40 (6) (2013) 065001. 1207.5194. https://doi.org/10.1088/0954-3899/40/6/065001
[20] M. Farina, C. Grojean, E. Salvioni, (Dys)Zphilia or a custodial breaking Higgs at the LHC, JHEP 2012 (7) (2012) 1–18. 1205.0011. https://doi.org/10.1007/JHEP07(2012)012
[21] J. Butterworth, H. Debnath, P. Fileviez Pérez, F. Mitchell, Custodial symmetry breaking and Higgs boson signatures at the LHC, Phys. Rev. D 109 (9) (2024) 095014. 2309.10027. https://doi.org/10.1103/PhysRevD.109.095014
[22] ATLAS Collaboration, Measurements of Higgs boson production via gluon–gluon fusion and vector-boson fusion using $H \to WW^* \to \ell\nu\ell\nu$ decays in pp collisions with the ATLAS detector and their effective field theory interpretations (2025). 2504.07686
[23] ATLAS Collaboration, The ATLAS Experiment at the CERN Large Hadron Collider, JINST 3 (2008) S08003. https://doi.org/10.1088/1748-0221/3/08/S08003
[24] L. Evans, P. Bryant, LHC Machine, JINST 3 (2008) S08001. https://doi.org/10.1088/1748-0221/3/08/S08001
[25] G. Avoni, et al., The new LUCID-2 detector for luminosity measurement and monitoring in ATLAS, JINST 13 (2018) P07017. https://doi.org/10.1088/1748-0221/13/07/P07017
[26] ATLAS Collaboration, Performance of the ATLAS trigger system in 2015, Eur. Phys. J. C 77 (2017) 317. 1611.09661. https://doi.org/10.1140/epjc/s10052-017-4852-3
[27] ATLAS Collaboration, Software and computing for Run 3 of the ATLAS experiment at the LHC, Eur. Phys. J. C 85 (2025) 234. 2404.06335. https://doi.org/10.1140/epjc/s10052-024-13701-w
[28] ATLAS Collaboration, Performance of the ATLAS muon triggers in Run 2, JINST 15 (2020) P09015. 2004.13447. https://doi.org/10.1088/1748-0221/15/09/p09015
[29] ATLAS Collaboration, Performance of electron and photon triggers in ATLAS during LHC Run 2, Eur. Phys. J. C 80 (2020) 47. 1909.00761. https://doi.org/10.1140/epjc/s10052-019-7500-2
[30] ATLAS Collaboration, The ATLAS inner detector trigger performance in pp collisions at 13 TeV during LHC Run 2, Eur. Phys. J. C 82 (2022) 206. 2107.02485. https://doi.org/10.1140/epjc/s10052-021-09920-0
[31] ATLAS Collaboration, ATLAS data quality operations and performance for 2015–2018 data-taking, JINST 15 (2020) P04003. 1911.04632. https://doi.org/10.1088/1748-0221/15/04/P04003
[32] ATLAS Collaboration, Luminosity determination in pp collisions at $\sqrt{s} = 13$ TeV using the ATLAS detector at the LHC, Eur. Phys. J. C 83 (2023) 982. 2212.09379. https://doi.org/10.1140/epjc/s10052-023-11747-w
[33] ATLAS and CMS Collaborations, Combined Measurement of the Higgs Boson Mass in pp Collisions at $\sqrt{s} = 7$ and 8 TeV with the ATLAS and CMS Experiments, Phys. Rev. Lett. 114 (2015) 191803. 1503.07589. https://doi.org/10.1103/PhysRevLett.114.191803
[34] E. Bothmann, et al., Event generation with Sherpa 2.2, SciPost Phys. 7 (3) (2019) 034. 1905.09127. https://doi.org/10.21468/SciPostPhys.7.3.034
[35] F. Cascioli, P. Maierhöfer, S. Pozzorini, Scattering Amplitudes with Open Loops, Phys. Rev. Lett. 108 (2012) 111601. 1111.5206. https://doi.org/10.1103/PhysRevLett.108.111601
[36] A. Denner, S. Dittmaier, L. Hofer, COLLIER: a fortran-based complex one-loop library in extended regularizations, Comput. Phys. Commun. 212 (2017) 220–238. 1604.06792. https://doi.org/10.1016/j.cpc.2016.10.013

[37] F. Buccioni, S. Pozzorini, M. Zoller, On-the-fly reduction of open loops, Eur. Phys. J. C 78 (1) (2018) 70. 1710.11452. https://doi.org/10.1140/epjc/s10052-018-5562-1

[38] F. Buccioni, J.N. Lang, J.M. Lindert, P. Maierhöfer, S. Pozzorini, H. Zhang, M.F. Zoller, OpenLoops 2, Eur. Phys. J. C 79 (10) (2019) 866. 1907.13071. https://doi.org/10.1140/epjc/s10052-019-7306-2

[39] P. Nason, A new method for combining NLO QCD with shower Monte Carlo algorithms, JHEP 11 (2004) 040. hep-ph/0409146. https://doi.org/10.1088/1126-6708/2004/11/040

[40] S. Frixione, P. Nason, C. Oleari, Matching NLO QCD computations with parton shower simulations: the POWHEG method, JHEP 11 (2007) 070. 0709.2092. https://doi.org/10.1088/1126-6708/2007/11/070

[41] S. Alioli, P. Nason, C. Oleari, E. Re, A general framework for implementing NLO calculations in shower Monte Carlo programs: the POWHEG BOX, JHEP 06 (2010) 043. 1002.2581. https://doi.org/10.1007/JHEP06(2010)043

[42] S. Alioli, S.F. Ravasio, J.M. Lindert, R. Röntsch, Four-lepton production in gluon fusion at NLO matched to parton showers, Eur. Phys. J. C 81 (8) (2021) 687. 2102.07783. https://doi.org/10.1140/epjc/s10052-021-09470-5

[43] J. Alwall, R. Frederix, S. Frixione, V. Hirschi, F. Maltoni, O. Mattelaer, H.S. Shao, T. Stelzer, P. Torrielli, M. Zaro, The automated computation of tree-level and next-to-leading order differential cross sections, and their matching to parton shower simulations, JHEP 07 (2014) 079. 1405.0301. https://doi.org/10.1007/JHEP07(2014)079

[44] T. Sjöstrand, S. Ask, J.R. Christiansen, R. Corke, N. Desai, P. Ilten, S. Mrenna, S. Prestel, C.O. Rasmussen, P.Z. Skands, An introduction to PYTHIA 8.2, Comput. Phys. Commun. 191 (2015) 159. 1410.3012. https://doi.org/10.1016/j.cpc.2015.01.024

[45] C. Anastasiou, K. Melnikov, F. Petriello, Fully differential Higgs boson production and the di-photon signal through next-to-next-to-leading order, Nucl. Phys. B 724 (2005) 197–246. hep-ph/0501130. https://doi.org/10.1016/j.nuclphysb.2005.06.036

[46] M. Grazzini, S. Kallweit, M. Wiesemann, Fully differential NNLO computations with MATRIX, Eur. Phys. J. C 78 (7) (2018) 537. 1711.06631. https://doi.org/10.1140/epjc/s10052-018-5771-7

[47] S. Catani, M. Grazzini, Next-to-Next-to-Leading-Order Subtraction Formalism in Hadron Collisions and its Application to Higgs-Boson Production at the Large Hadron Collider, Phys. Rev. Lett. 98 (2007) 222002. hep-ph/0703012. https://doi.org/10.1103/PhysRevLett.98.222002

[48] C. Anastasiou, C. Duhr, F. Dulat, F. Herzog, B. Mistlberger, Higgs Boson Gluon-Fusion Production in QCD at Three Loops, Phys. Rev. Lett. 114 (2015) 212001. 1503.06056. https://doi.org/10.1103/PhysRevLett.114.212001

[49] NNPDF Collaboration, R.D. Ball, et al., Parton distributions for the LHC run II, JHEP 04 (2015) 040. 1410.8849. https://doi.org/10.1007/JHEP04(2015)040

[50] ATLAS Collaboration, ATLAS Pythia 8 tunes to 7 TeV data, ATL-PHYS-PUB-2014-021, 2014. https://cds.cern.ch/record/1966419.

[51] A. Denner, and R. Franken, and T. Schmidt, and C. Schwan, NLO QCD and EW corrections to vector-boson scattering into W^+W^- at the LHC, JHEP 11 (2022) 098. 2202.10844. https://doi.org/{10.1007/jhep06(2022)098}

[52] H.B. Hartanto, B. Jäger, L. Reina, D. Wackeroth, Higgs boson production in association with top quarks in the POWHEG BOX, Phys. Rev. D 91 (9) (2015) 094003. 1501.04498. https://doi.org/10.1103/PhysRevD.91.094003

[53] P. Nason, C. Oleari, NLO Higgs boson production via vector-boson fusion matched with shower in POWHEG, JHEP 02 (2010) 037. 0911.5299. https://doi.org/10.1007/JHEP02(2010)037

[54] G. Luisoni, P. Nason, C. Oleari, F. Tramontano, $HW^{\pm}/HZ$ + 0 and 1 jet at NLO with the POWHEG BOX interfaced to GoSam and their merging within MiNLO, JHEP 10 (2013) 083. 1306.2542. https://doi.org/10.1007/JHEP10(2013)083

[55] S. Frixione, G. Ridolfi, P. Nason, A positive-weight next-to-leading-order Monte Carlo for heavy flavour hadroproduction, JHEP 09 (2007) 126. 0707.3088. https://doi.org/10.1088/1126-6708/2007/09/126

[56] ATLAS Collaboration, Measurement of the Z/γ^* boson transverse momentum distribution in pp collisions at $\sqrt{s} = 7$ TeV with the ATLAS detector, JHEP 09 (2014) 145. 1406.3660. https://doi.org/10.1007/JHEP09(2014)145

[57] J. Butterworth, et al., PDF4LHC recommendations for LHC Run II, J. Phys. G 43 (2016) 023001. 1510.03865. https://doi.org/10.1088/0954-3899/43/2/023001

[58] T. Gleisberg, S. Höche, Comix, a new matrix element generator, JHEP 12 (2008) 039. 0808.3674. https://doi.org/10.1088/1126-6708/2008/12/039

[59] C. Anastasiou, L. Dixon, K. Melnikov, F. Petriello, High-precision QCD at hadron colliders: Electroweak gauge boson rapidity distributions at next-to-next-to leading order, Phys. Rev. D 69 (2004) 094008. hep-ph/0312266. https://doi.org/10.1103/PhysRevD.69.094008

[60] S. Schumann, F. Krauss, A parton shower algorithm based on Catani–Seymour dipole factorisation, JHEP 03 (2008) 038. 0709.1027. https://doi.org/10.1088/1126-6708/2008/03/038

[61] S. Catani, F. Krauss, B.R. Webber, R. Kuhn, QCD Matrix Elements + Parton Showers, JHEP 11 (2001) 063. hep-ph/0109231. https://doi.org/10.1088/1126-6708/2001/11/063

[62] S. Höche, F. Krauss, S. Schumann, F. Siegert, QCD matrix elements and truncated showers, JHEP 05 (2009) 053. 0903.1219. https://doi.org/10.1088/1126-6708/2009/05/053

[63] S. Höche, F. Krauss, M. Schönherr, F. Siegert, A critical appraisal of NLO + PS matching methods, JHEP 09 (2012) 049. 1111.1220. https://doi.org/10.1007/JHEP09(2012)049

[64] S. Höche, F. Krauss, M. Schönherr, F. Siegert, QCD matrix elements + parton showers. The NLO case, JHEP 04 (2013) 027. 1207.5030. https://doi.org/10.1007/JHEP04(2013)027

[65] S. Kallweit, J.M. Lindert, P. Maierhöfer, S. Pozzorini, M. Schönherr, NLO electroweak automation and precise predictions for W + multijet production at the LHC, JHEP 04 (2015) 012. 1412.5157. https://doi.org/10.1007/JHEP04(2015)012

[66] M. Bähr, et al., Herwig++ physics and manual, Eur. Phys. J. C 58 (2008) 639. 0803.0883. https://doi.org/10.1140/epjc/s10052-008-0798-9

[67] J. Bellm, et al., Herwig 7.0/Herwig++ 3.0 release note, Eur. Phys. J. C 76 (4) (2016) 196. 1512.01178. https://doi.org/10.1140/epjc/s10052-016-4018-8

[68] L.A. Harland-Lang, A.D. Martin, P. Motylinski, R.S. Thorne, Parton distributions in the LHC era: MMHT 2014 PDFs, Eur. Phys. J. C 75 (5) (2015) 204. 1412.3989. https://doi.org/10.1140/epjc/s10052-015-3397-6

[69] ATLAS Collaboration, Studies on Top-Quark Monte Carlo Modelling for Top2016, ATL-PHYS-PUB-2016-020, 2016. https://cds.cern.ch/record/2216168.

[70] NNPDF Collaboration, R.D. Ball, et al., Parton distributions with LHC data, Nucl. Phys. B 867 (2013) 244. 1207.1303. https://doi.org/10.1016/j.nuclphysb.2012.10.003

[71] M. Czakon, D. Heymes, A. Mitov, D. Pagani, I. Tsinikos, M. Zaro, Top-pair production at the LHC through NNLO QCD and NLO EW, JHEP 10 (2017) 186. 1705.04105. https://doi.org/10.1007/JHEP10(2017)186

[72] M. Beneke, P. Falgari, S. Klein, C. Schwinn, Hadronic top-quark pair production with NNLL threshold resummation, Nucl. Phys. B 855 (2012) 695–741. 1109.1536. https://doi.org/10.1016/j.nuclphysb.2011.10.021

[73] M. Cacciari, M. Czakon, M. Mangano, A. Mitov, P. Nason, Top-pair production at hadron colliders with next-to-next-to-leading logarithmic soft-gluon resummation, Phys. Lett. B 710 (2012) 612–622. 1111.5869. https://doi.org/10.1016/j.physletb.2012.03.013

[74] M. Czakon, A. Mitov, Top++: A program for the calculation of the top-pair cross-section at hadron colliders, Comput. Phys. Commun. 185 (2014) 2930. 1112.5675. https://doi.org/10.1016/j.cpc.2014.06.021

[75] P. Bärnreuther, M. Czakon, A. Mitov, Percent-Level-Precision Physics at the Tevatron: Next-to-Next-to-Leading Order QCD Corrections to $q\bar{q} \to t\bar{t} + X$, Phys. Rev. Lett. 109 (2012) 132001. 1204.5201. https://doi.org/10.1103/PhysRevLett.109.132001

[76] M. Czakon, A. Mitov, NNLO corrections to top-pair production at hadron colliders: the all-fermionic scattering channels, JHEP 12 (2012) 054. 1207.0236. https://doi.org/10.1007/JHEP12(2012)054

[77] M. Czakon, A. Mitov, NNLO corrections to top pair production at hadron colliders: the quark-gluon reaction, JHEP 01 (2013) 080. 1210.6832. https://doi.org/10.1007/JHEP01(2013)080

[78] M. Czakon, P. Fiedler, A. Mitov, Total Top-Quark Pair-Production Cross Section at Hadron Colliders Through $O(\alpha_S^4)$, Phys. Rev. Lett. 110 (2013) 252004. 1303.6254. https://doi.org/10.1103/PhysRevLett.110.252004

[79] E. Re, Single-top Wt-channel production matched with parton showers using the POWHEG method, Eur. Phys. J. C 71 (2011) 1547. 1009.2450. https://doi.org/10.1140/epjc/s10052-011-1547-z

[80] S. Frixione, E. Laenen, P. Motylinski, C. White, B.R. Webber, Single-top hadroproduction in association with a W boson, JHEP 07 (2008) 029. 0805.3067. https://doi.org/10.1088/1126-6708/2008/07/029

[81] N. Kidonakis, Two-loop soft anomalous dimensions for single top quark associated production with a W^- or H^-, Phys. Rev. D 82 (2010) 054018. 1005.4451. https://doi.org/10.1103/PhysRevD.82.054018

[82] N. Kidonakis, Top quark production, in: Proceedings, Helmholtz International Summer School on Physics of Heavy Quarks and Hadrons (HQ2013), 2013, pp. 139–168. 1311.0283. https://doi.org/10.3204/DESY-PROC-2013-03/Kidonakis

[83] ATLAS Collaboration, The ATLAS Simulation Infrastructure, Eur. Phys. J. C 70 (2010) 823. 1005.4568. https://doi.org/10.1140/epjc/s10052-010-1429-9

[84] S. Agostinelli, et al., GEANT4 – a simulation toolkit, Nucl. Instrum. Meth. A 506 (2003) 250. https://doi.org/10.1016/S0168-9002(03)01368-8

[85] T. Sjöstrand, S. Mrenna, P. Skands, A brief introduction to PYTHIA 8.1, Comput. Phys. Commun. 178 (2008) 852–867. 0710.3820. https://doi.org/10.1016/j.cpc.2008.01.036

[86] ATLAS Collaboration, The Pythia 8 A3 tune description of ATLAS minimum bias and inelastic measurements incorporating the Donnachie–Landshoff diffractive model, ATL-PHYS-PUB-2016-017, 2016. https://cds.cern.ch/record/2206965.

[87] ATLAS Collaboration, Electron and photon performance measurements with the ATLAS detector using the 2015–2017 LHC proton–proton collision data, JINST 14 (2019) P12006. 1908.00005. https://doi.org/10.1088/1748-0221/14/12/P12006

[88] ATLAS Collaboration, Muon reconstruction and identification efficiency in ATLAS using the full Run 2 pp collision data set at $\sqrt{s} = 13$ TeV, Eur. Phys. J. C 81 (2021) 578. 2012.00578. https://doi.org/10.1140/epjc/s10052-021-09233-2

[89] ATLAS Collaboration, Electron and photon efficiencies in LHC Run 2 with the ATLAS experiment, JHEP 05 (2024) 162. 2308.13362. https://doi.org/10.1007/JHEP05(2024)162

[90] ATLAS Collaboration, Evidence for the associated production of the Higgs boson and a top quark pair with the ATLAS detector, Phys. Rev. D 97 (2018) 072003. 1712.08891. https://doi.org/10.1103/PhysRevD.97.072003

[91] M. Cacciari, G.P. Salam, G. Soyez, The anti-k_t jet clustering algorithm, JHEP 04 (2008) 063. 0802.1189. https://doi.org/10.1088/1126-6708/2008/04/063

[92] M. Cacciari, G.P. Salam, G. Soyez, FastJet user manual, Eur. Phys. J. C 72 (2012) 1896. 1111.6097. https://doi.org/10.1140/epjc/s10052-012-1896-2

[93] ATLAS Collaboration, Jet reconstruction and performance using particle flow with the ATLAS Detector, Eur. Phys. J. C 77 (2017) 466. 1703.10485. https://doi.org/10.1140/epjc/s10052-017-5031-2

[94] ATLAS Collaboration, Jet energy scale measurements and their systematic uncertainties in proton–proton collisions at $\sqrt{s} = 13$ TeV with the ATLAS detector, Phys.

Rev. D 96 (2017) 072002. 1703.09665. https://doi.org/10.1103/PhysRevD.96.072002

[95] ATLAS Collaboration, Identification and rejection of pile-up jets at high pseudo-rapidity with the ATLAS detector, Eur. Phys. J. C 77 (2017) 580. 1705.02211. https://doi.org/10.1140/epjc/s10052-017-5081-5

[96] ATLAS Collaboration, Forward jet vertex tagging using the particle flow algorithm, ATL-PHYS-PUB-2019-026, 2019. https://cds.cern.ch/record/2683100.

[97] ATLAS Collaboration, ATLAS b-jet identification performance and efficiency measurement with $t\bar{t}$ events in pp collisions at $\sqrt{s} = 13$ TeV, Eur. Phys. J. C 79 (2019) 970. 1907.05120. https://doi.org/10.1140/epjc/s10052-019-7450-8

[98] ATLAS Collaboration, Selection of jets produced in 13 TeV proton–proton collisions with the ATLAS detector, ATLAS-CONF-2015-029, 2015. https://cds.cern.ch/record/2037702.

[99] ATLAS Collaboration, The performance of missing transverse momentum reconstruction and its significance with the ATLAS detector using 140 fb^{-1} of $\sqrt{s} = 13$ TeV pp collisions, Eur. Phys. J. C 85 (2025) 606. 2402.05858. https://doi.org/10.1140/epjc/s10052-025-14062-8

[100] M. Abadi, et al., TensorFlow: Large-Scale Machine Learning on Heterogeneous Distributed Systems, 2015. Software available from tensorflow.org, https://www.tensorflow.org/.

[101] R. Kohavi, et al., A Study of Cross-Validation and Bootstrap for Accuracy Estimation and Model Selection, in: Ijcai, 14, Montreal, Canada, 1995, pp. 1137–1145.

[102] T. Plehn, D. Rainwater, D. Zeppenfield, A Method for identifying $H \to \tau^+\tau^- \to e^\pm\mu^\mp/p_T$ at the CERN LHC, Phys. Rev. D 61 (9) (2000) 093005. hep-ph/9911385. https://doi.org/10.1103/PhysRevD.61.093005

[103] K. Lehmann, B. Stelzer, The Fake Factor Method and its relation to the Matrix Method, Nucl. Instrum. Meth. A 1054 (2023) 168376. https://doi.org/10.1016/j.nima.2023.168376

[104] ATLAS Collaboration, Studies of $t\bar{t}/tW$ interference effects in $b\bar{b}\ell^+\ell^{-\prime}\nu\bar{\nu}'$ final states with POWHEG and MADGRAPH5_AMC@NLO setups, ATL-PHYS-PUB-2021-042, 2021. https://cds.cern.ch/record/2792254.

[105] ATLAS Collaboration, Measurements of WH and ZH production with Higgs boson decays into bottom quarks and direct constraints on the charm Yukawa coupling in 13 TeV pp collisions with the ATLAS detector, JHEP 04 (2025) 075. 2410.19611. https://doi.org/10.1007/JHEP04(2025)075

[106] G. Cowan, K. Cranmer, E. Gross, O. Vitells, Asymptotic formulae for likelihood-based tests of new physics, Eur. Phys. J. C 71 (2011) 1554. 1007.1727. https://doi.org/10.1140/epjc/s10052-011-1554-0

[107] S.S. Wilks, The Large-Sample Distribution of the Likelihood Ratio for Testing Composite Hypotheses, Ann. Math. Statist. 9 (1) (1938) 60–62.

[108] J. Neyman, Outline of a Theory of Statistical Estimation Based on the Classical Theory of Probability, Phil. Trans. Roy. Soc. Lond. A 236 (767) (1937) 767.

[109] ATLAS Collaboration, Evidence of off-shell Higgs boson production from ZZ leptonic decay channels and constraints on its total width with the ATLAS detector, Phys. Lett. B 846 (2023) 138223. 2304.01532. https://doi.org/10.1016/j.physletb.2023.138223

[110] ATLAS Collaboration, ATLAS Computing Acknowledgements, ATL-SOFT-PUB-2025-001, 2025. https://cds.cern.ch/record/2922210.